NTNU – Trondheim
Norwegian University of
Science and Technology

Transverse tensile armour buckling of flexible pipes

chongyao Zhou

Marine Technology
Submission date: June 2014
Supervisor: Svein Sævik, IMT
Co-supervisor: Naiquan Ye, Marintek

Norwegian University of Science and Technology
Department of Marine Technology

NTNU – Trondheim
Norwegian University of
Science and Technology

Transverse Tensile Armour Buckling of Flexible Pipes

Chongyao Zhou

June 2014

MASTER THESIS

Department of Marine Technology

Faculty of Engineer Science and Technology

Norwegian University of Science and Technology

Supervisor 1: Professor Svein Sævik

Supervisor 2: Doctor Naiquan Ye

Preface

This master thesis lasts for two semesters in total, including the literature study of flexible pipe technology, the introduction of failure modes and design criteria, and the FE software study. The theory of non-linear finite element method and the modelling method in Bflex2010 are introduced as well as the analytical solution for the transverse buckling problem.

The analysis works are carried out in Bflex2010 to perform the analysis of tensile layers transverse buckling behaviour of the flexible risers caused by the couple effect of compression and bending, especially the cyclic bending. Two finite element models are built to simulate the transverse buckling mechanism under different loading conditions. The effect of anti-buckling tape is also studied, including the sensitivity study of the lay angle direction of anti-buckling tape to the transverse buckling behaviour.

Trondheim, June 2014

.....

Chongyao Zhou

Acknowledgment

The main work of this thesis is carried out in the finite element software Bflex2010. Through the study of the software and the relevant theory, I have achieved a lot of knowledge and experience in research and analysis work. However, it is more difficult to understand the theory behind the software relevant to non-linear finite element method than to use the software itself.

Here I will give my special thanks to professor Svein Sævik for his kindly help for my thesis. His erudition, preciseness, innovative ideas and the encourage he gave to me also inspired me and had a great impact on me during the work! Another special thanks will give to the senior scientist researcher Naiquan Ye in MARINTEK for his thoughtful and thorough guidance during the master thesis, especially for the application knowledge of Bflex2010 and the weekly guidance meeting for answering questions and introducing theory background knowledge. I will thank both of them not only for the great knowledge of the theory behind the thesis and operation with Bflex2010, but also for the process to study and research! I will also give my special thanks to scientist researcher Guomin Ji in MARINTEK, for his generous and kindness to help me to run my programs in the serve in MARINTEK for almost one months, and the valuable and priceless guidances from him about the master thesis. I will also give my thanks to my classmates for their help and thoughtful ideas.

Trondheim, June 2014

Chongyao Zhou

Summary and Conclusions

During the installation and operation process, the empty flexible pipe will experience a large end fitting load which is the compression load at the ends of the pipe. At the same time, the dynamic load from wave and current will force the pipe to bend cyclically which will cause the transverse buckling within the tensile layers. The end of pipe will rotate due to the transverse buckling mechanism during each cycle, resulting in a serious end rotation to make the pipe collapse. This thesis will study transverse buckling behaviour under different loading conditions and perform the sensitivity analysis to study the influence of the relevant characteristic parameters.

This section will briefly summarize the main contents and conclusions in the thesis.

- INTRODUCTION

Chapter 1 is the introduction of the master thesis, including the study motivation, previous literature overview about this topic, the main contributions of this thesis and the structure of the rest thesis.

- LITERATURE STUDY

Chapter 2 and Chapter 3 are the literature study, focusing on the flexible pipe technology, failure modes and design criteria. Chapter 2 includes an introduction to the flexible pipe applications in the offshore industry, flexible pipe structure and termination of riser. Chapter 3 is a brief introduction of failure modes and design criteria.

- THEORY AND METHOD

Chapter 4 is an introduction to the linear finite element methods and non-linear finite element methods and the relevant non-linear code used in FEM software, Bflex2010 and Marc. The theory background of the finite element model established in Bflex2010 and the analytical methods for stress and buckling analysis in tensile armour are also shown in this chapter. The physical interpretation of the lateral buckling failure mode is shown as well.

- MODEL ESTABLISHMENT

Chapter 5 is an introduction of the model establishment, including the simplified model(one tendon without friction) and the full model(all the layers including anti-buckling tape). The determination of loading conditions, boundary conditions and relevant important parameters are also introduced.

- BUCKLING PERFORMANCE STUDY OF SIMPLIFIED MODEL

Chapter 6 is the lateral buckling study of the simplified model, including the influence of lay angle, start angle and imperfection. Three sensitivity studies for the time interval, axisymmetric interaction and start procedure in Bflex2010 are also carried out.

Lay angle will have a big influence on the buckling occurring positions during the process of loading, but it is hard to predict. However, the buckling load capacity will be increased due to the decrease of lay angle, which is testified by the analytical solution and tests in Bflex2010. The start angle will have no influence on the buckling load capacity except the buckling occurring positions. The imperfection will lead to a sudden axial force increase in the tendon which is shown as a snap in the realistic physical issues. This phenomenon will be presented and explained in the thesis.

For the sensitivity study, the following conclusions can be obtained: 1) The length of time interval will decide the accuracy of the test in Bflex2010. The smaller time interval will capture the buckling behavior at the beginning of the process. 2) The axisymmetric interaction and start procedure will not have a significant influence on the test results.

- BUCKLING PERFORMANCE STUDY OF FULL MODEL

Chapter 7 is the lateral buckling study of the full model, including the comparison with the simplified model under the same load conditions, the detail study of the lateral buckling of tendons and the end rotation of riser caused by lateral buckling due to the cyclic bending.

The results of full model are also close to the analytical solution and a little more conservative than the simplified model. The end rotation behaviour due to transverse buckling is studied by full model, which can simulate the failure modes in a right way and the results will be close to the experimental results if the additional axial stiffness of pipes in experiments is provided.

The sensitivity study is performed to study the effect of anti-buckling tape. The results show that the anti-buckling tape has a large effect to prevent the transverse buckling and the lay angle

direction of the anti-buckling tape will also affect the transverse buckling behaviour and prevent the buckling process to a great extent.

- CONCLUSIONS

Chapter 8 illustrates the main conclusions from this thesis, the discussion of the results and the recommendation for further work. The further work should focus on the study of the anti-buckling tape effect, as a function of material, lay angle and tape cross-section.

Scope of work

The local buckling of flexible pipe due to the over bending and tension can be divided into two different types: radial buckling and lateral buckling. In this thesis, a study and analysis of lateral buckling is carried out based on the computer code in Marintek software Bflex2010 and the scope of work is shown below:

1) Literature study about flexible pipe technology, failure modes and design criteria; non-linear finite element methods relevant for non-linear FEM codes: MARC and Bflex2010; analytical methods for stress and buckling analysis of flexible pipes.

2) Bflex modelling of pipe with one tendon under no friction for analysing the lateral tensile armour buckling failure mode.

3) Study the influence of start angle and lay angle to the lateral buckling.

4) Sensitivity study for three factors: time interval, axisymmetric interaction and start procedure in Bflex2010.

5) Compare with the results from analytical equations, including buckling load and post-buckling load.

6) Bflex modelling of pipe with all the layers including anti-buckling tape with friction for analysing the lateral tensile armour buckling failure mode.

7) Compare the results between simplified model and full model. Study the influence of friction and anti-buckling tape.

8) Study the lateral buckling behaviour of three flexible pipes under different compressions and cyclic bending. Sensitivity analysis is carried out to study the influence of the anti-buckling tape and the inverse lay angle of anti-buckling tape.

9) Conclusions, results discussion and recommendations for further work.

Contents

List of Figures

List of Tables

Nomenclature

Roman Letters

$\mathbf{a}^e$	Connectivity matrix
A_t	Tensile layer cross-section area
A_j	Pipe cross-section area
b	Width of the tendon
BVP	Matlab Solver-Boundary Value problem
Dof	Degree of freedom
$\mathbf{D}$	Linear elastic transform matrix
E	Young's module
E_{11}	Green strain tensor in curve linear coordinates
E_{xx}	longitudinal Green strain
$\mathbf{f}$	Volume force vector
F_f	Fill factor
g	Current gap at the time $t+\Delta t$
G	Shear module
G_m	Metric
i	Iteration number
I	Moment inertia
I_1, I_2, I_3	Moment inertia respect to three axial
$\mathbf{I}_i$	Base vectors in global coordinate system
$\mathbf{j}_i$	Base vectors in local beam element system
$\mathbf{k}$	Element stiffness matrix
$\mathbf{k}_{Ti}$	Element stiffness matrix
$\mathbf{K}$	System stiffness matrix
$\mathbf{K}_T$	Global tangential stiffness matrix
l	Pipe length
l_e	Buckling length

L_0	Initial strain
M_1, M_2, M_3	Local moments respect to the axis in local coordinate system
n	Number of wires in the layer
$\mathbf{n}$	Outward surface normal vector of body
P	Buckling load
q_3	Contact line load in the radial direction
Q_1, Q_2, Q_3	Local shear forces respect to the axis in local coordinate system
$\Delta\mathbf{r}$	Change of nodal displacement vector
$\mathbf{r}$	Nodal displacement vector
R	Tensile layer radial
$\mathbf{R}^c$	Vector of concentrated nodal point forces
$\mathbf{R}^o$	Vector of element nodal forces
$\Delta\mathbf{R}$	Load increment
$\mathbf{S}$	General element nodal point forces
$\mathbf{S^0}$	Element nodal point force
$\Delta\mathbf{S}_i$	Element load vector
t_{tot}	Total thickness for two layers
t	Tendon thickness
T_e	True wall tension
T_w	Effect tension
Δt	Time increment
$\Delta\mathbf{T}_i$	Global system transformation matrix
$\mathbf{u}_0, u_{i_0}$	Displacement vector of wire center line and its component in direction i
$\mathbf{u}, u_i$	Displacement vector and its component in direction i
$\mathbf{u}$	Displacement vector
$u_{i,j}$	Differentiation of the displacement components
u_i	Displacement components along the axis
$\Delta\mathbf{u}$	Increment in displacement associated to an time interval $[t, t+\Delta t]$
$\mathbf{v}$	Element displacement vector X_i
X_1, X_2, X_3	Local coordinate system respect to the axis

Greek Letters

α	Lay angle
Δ	Differential operator matrix
θ_i	Rotation degree about local coordinates x, y, z
θ	Start angle
ϵ_1	1st order axial strain
ϵ_2	Centre line rotation about the X_3 axis
ϵ_3	Centre line rotation about the X_2 axis
ω_1	Torsion of the centre line
ω_2	The curvatures about the X_2 axis
ω_3	The curvatures about the X_3 axis
ω_{ip}	The prescribed torsion and curvature quantities from bending
ε_{ij}	Strain quantities refer to the Z^i axis and X^j axis
σ	Stress components
σ_{xx}	Longitude stress in HSHEAR363
$\sigma_{11}, \sigma_{22}, \sigma_{33}$	Normal stress components
$\sigma_{12}, \sigma_{23}, \sigma_{13}$	Shear stress components
σ_{11j}	Axial stress of the layer
κ_1	Initial torsion
κ_2	Normal curvature
κ_3	Transverse curvature
κ_t	Cylinder curvature in tendon transverse direction
κ_i	Initial torsion and curvatures respect to i direction

Chapter 1

INTRODUCTION

Flexible pipe has been widely used in subsea and offshore industry for many years. In the oil and gas transportation industry, flexible pipe and riser are playing an important role that will result in a higher design standard of the structure of flexible pipe. However, there will be several failure modes occurring during the operation of flexible pipe, especially in the very harsh environment. The complicated hydrodynamic response and the unpredicted operation accidents will challenge the design and production standards in a great extent.

A basic floating production system with the riser system is shown in Fig.1.1.

Figure 1.1: Flexible riser system

1.1 Motivation

Flexible pipe is an unbonded steel-polymer composite structure comprised by several different layers. And the two helix tensile layers are responsible for providing the longitudinal load capacity. During the pipe laying process in the deep water, the flexible pipe is free hanged from the piping vessel to the seabed and it will be empty during this process, which will introduce the large hydrostatic longitudinal pressure to the end of pipe. In addition, the pipe will also bear the cyclic bending due to the waves, currents and the motion of the piping vessel.

The compression and cyclic bending will lead to the instability of the tensile armours in both lateral and radial directions. Furthermore, if the anti-buckling tape is assumed strong enough, the inner tensile armour will lose the stability in lateral direction first due to the decreasing of friction and the gap between the two tensile layers during the process. This will introduce the lateral buckling of the tensile armour, and in order to keep the torsion balance between the inner and outer tensile layers, the flexible pipe will experience a sever twist during the cyclic bending which will lead to many other failure modes, and result in very serious operation accidents.

This kind of accident happens so frequently and seriously that it is important and necessary to analyse and study this phenomenon in a much better way.

1.2 Literature Survey

Transverse buckling failure mode has been studied for several years but few papers concerning about it in the open literatures. The mechanism of this failure mode was first introduced and described by Braga and Kaleff[8], based on the experimental results, which rebuilding the lateral buckling failure mode for study and analysis. Further experiment to study the lateral buckling behaviour was carried by Philippe SECHER, Fabrice BECTARTE and Antoine FELIX-HENRY to study the flexible pipes under 3000m water depth[2], but the detail data were not given.

The lateral buckling behaviour due to the cyclic bending is studied by Niels H. Østergaard, Anders Lyckegaard and Jens J. Andreasen[9]. The experiments were also carried out to compare with the results from theoretical analytical solution based on the simplified modelling approaches given by Østergaard[10] [4]. However, the simplified modelling approaches only included one tendon under no friction, in order to study the influence of the friction and anti-

buckling tape and the end rotation due to cyclic bending, a full model should be established to capture and predict this failure mode. Furthermore, the effect factors relative to the lateral buckling mechanism should also be researched, such as lay angle and the cross section.

1.3 Main Contributions

The point of this master thesis is to study the lateral buckling failure mode of flexible pipe. The first part is to establish the simplified model based on the theory of Østergaard[9] to study the lateral buckling behaviour under different lay angles, cross-sections and imperfections.

The second part is to establish the full model including friction and anti-buckling tape in Bflex2010 based on the new elements and cross-section type developed by Svein Sævik[11][12], to study the lateral buckling mechanism due to cyclic bending and the influence of structural characters of anti-buckling tape. Three risers of different sizes are tested under different compression loads and number of bending cycles. The test results are compared with the data from the experiments carried out by Østergaard[9], to find out the difference and the corresponding reasons. The influence of anti-buckling tape is studied in this thesis, including the lay angle direction of anti-buckling tape effect to the transverse buckling problem. The theoretical reason about this influence is also explained.

1.4 Thesis Structure

The rest chapters of the thesis are structured as follows.

Chapter 2 gives an introduction to flexible pipe technology.

Chapter 3 gives a brief review of the failure modes and design criteria.

Chapter 4 is to introduce the theory background of the establishment of the finite element model in Bflex2010 .The analytical method as well as the analytical solution for the lateral buckling load are also introduced.

Chapter 5 is a description of the establishment method of the models in Bflex, including the simplified model and the full model, and the input data of the flexible risers for the tests. The loading conditions and the boundary conditions are also introduced in this chapter.

Chapter 6 studies the lateral buckling behaviour of the simplified model, and six cases including three sensitivity tests are carried out to study the transverse buckling process, the influence of lay angle, start angle, time increment, axisymmetric interaction and start procedure parameter to the lateral buckling mechanism.

Chapter 7 focuses on the lateral buckling behaviour of the full model. The comparison between simplified model and full model is carried out to study the influence of friction and anti-buckling tape. Three risers of different sizes are tested under different compression and cyclic bending, to study the lateral buckling mechanism due to the cyclic bending. The effect of anti-buckling tape is also studied, including the lay angle direction effect to the transverse buckling failure mode.

Chapter 8 illustrates the main findings, conclusions and results discussion as well as the recommendation further works.

Chapter 2

FLEXIBLE PIPE TECHNOLOGY

2.1 Introduction

This chapter is to give a brief overview of flexible pipe technology. According to the different functional requirements, there are many speciallzation areas to apply flexible pipe. Flexible pipe is designed as an unbonded steel-polymer composite structure comprised by several different layers with corresponding mechanical properities and structural functions in order to provide sufficient structural capacity against large tension, compression and torsion, external and internal pressure as well as large bending deflections. One advantage to use flexible pipe instead of steel pipe is that it provides an easy way to transport and install through prefabrication in long lengths and stored on reels. Another is the allowance to permanent connect between a floating support vessel with large motions and subsea structures.

2.2 Applications in Offshore Industry

According to the two aspects mentioned as two advantages above, the applications of flexible pipe are listed as followed:

- Flowlines for intra-field connection of wellheads, templates, loading terminals, ect.
- Riser system for connecting subsea installations with floating facilities, including the combined system flexible pipes used as jumper lines between rigid risers and platforms.

- Jumper lines between fixed and floating platforms.
- Loading hoses for offshore loading terminals.
- Small-diameter services lines, such as kill and choke lines, umbilicals, etc.

However, the main application is the riser system which has a multitude of functions. The riser system plays an important role in both production and drilling fields and the key functions are:

- Well product transportation for oil,gas and condensate
- Well control lines
- Injection of water and gas
- Processed product export

Different requirements for a riser system such as the flexible pipe number, sizes, pressure ratings and internal coating requirements depend on these functions above. If the rules for maintaining structural connection between subsea installation and surface vessel is concentrated on, the main requirements are:

- Water depth
- Motions of support vessel
- Current and wave loads

These parameters must be taken account into durning the riser system design process to make sure the external loading is kept in the acceptable limits range. These limits are tension, curvature, torsion, interference and compression.

Another important issue for designing a riser system is to choose the appropriate method. Some possible flexible riser configurations are illustrated in Fig.2.1. The main difference is the application of buoyancy modules and the anchoring methods.

As there is a strongly operational relationship between the riser system and support vessel, the design of them must be considered closely to determine the support point and the corresponding motions.

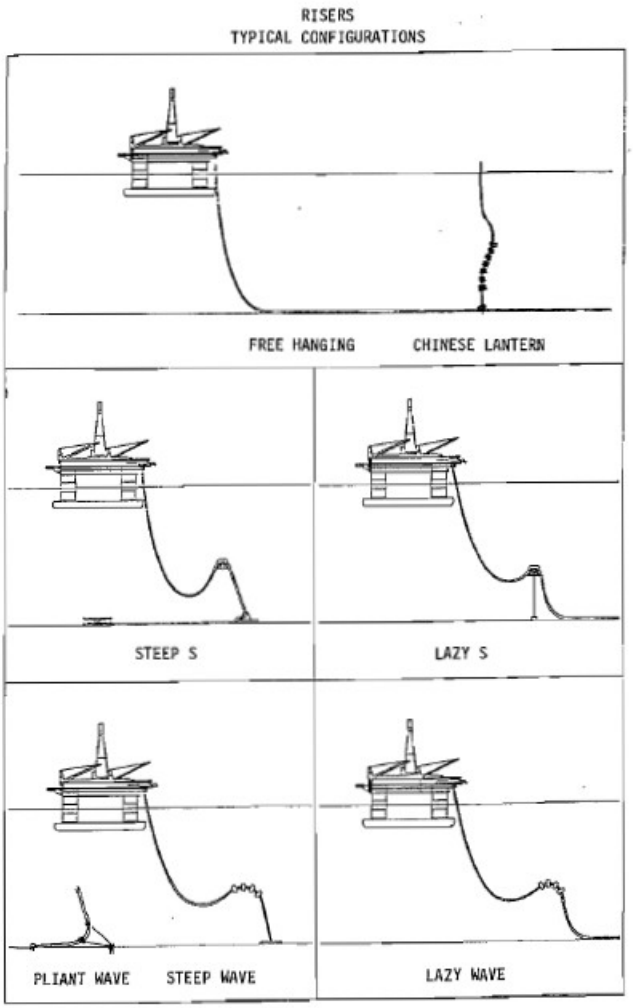

Figure 2.1: Flexible riser configurations[1]

2.3 Flexible Pipe Structure

As a composite structure with a number of layers, flexible pipe has two basic types of components. One is armour components which can provide pipe strength obtained by the spiral wire construction, another is sealing components providing fluid containment obtained by the polymer or compliant steel tubes.

According to the two basic component types, there are two pipe constructions in general, that is, nonbonded and bonded pipe structure. The mainly difference is the relative motion between the armour and sealing components. For the nonbonded structure, the relative slide is allowed because of the independent cylindrical layer type for the two components, while for the bonded structure, the relative motion is restrained since the two components are monolithic.

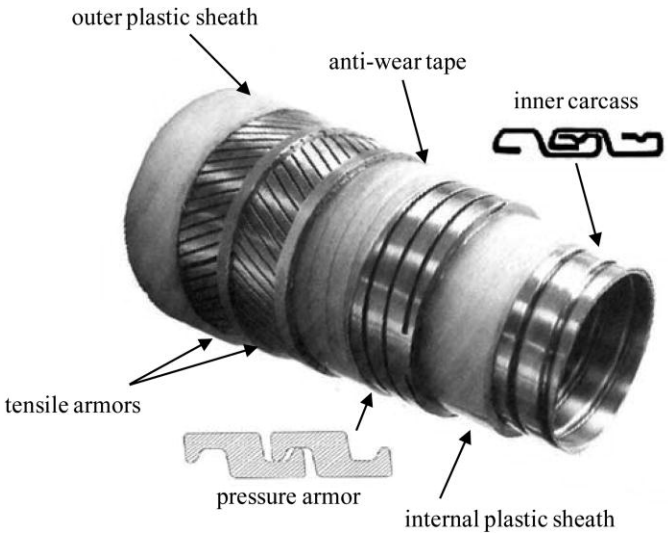

Figure 2.2: A typical flexible pipe cross section

When it comes to the short length piping industry, the bonded flexible pipe is mostly considered and the typical applications are jumper lines, loading hoses and kill/choke lines. While the unbounded flexible pipe can be used in long length piping industry and the length is up to several kilometres which can be applied in riser system. The unbounded flexible can be divided into two types: rough bore and smooth bore structures and the main difference is the application of steel carcass. In rough bore pipe, the carcass is used to support the inner liner and prevent its collapse, when the sudden pressure drop happens due to the injection of fluid. For the smooth bore pipe, no carcass inside, can only be used in the situation where is no gas diffusion through the internal thermoplastic layer. The cross section of flexible pipe is the vital characteristic and a typical cross section is shown in Fig.2.2.

- Carcass is to support the inner liner and provide strength due to the external pressure. It is built from an open interlocking profile and is not hermetic.
- Pressure armour is to provide strength to support loads due to both internal pressure and external pressure and is usually made of Z-layer or C-Clip layer.
- Tensile armour is to provide axial and torsional capacity and gives support to the pipe weight and transfer to the end termination point. It is made of flat rectangular wires with a layer angle of 30^o to 50^o and typically consists two layers with opposite directions.

- Inner and outer liner, namely the internal and external thermoplastic sheath, provides the sealing of internal transported fluids and seawater outside, protects the armours from corrosion. Another function is to bear high strain and high temperature.

- To reduce the friction of the metallic armour layers, the anti-wear layer is used for this function and also to separate these layers.

For the buckling problem which will be studied in deep in this thesis, a so called anti-buckling tape layer with high strength may be applied to support the armour in radial direction which is also necessary for tensile armour to resist axial loads.

2.4 Termination of Riser

One of the most critical parts of a flexible pipe is the termination point where the pipe is connected to a rigid structure. In this area, the flexible pipe will experience the over bending behaviour. To limit it, a bending stiffener is introduced to increase the bending stiffness of pipe in this area. Another way to deal with the over bending problem is to lead the pipe through a bellmouth, which cannot increase the bending stiffness but can limit the bending curvature. The two typical ways are illustrated in Fig.2.3 below.

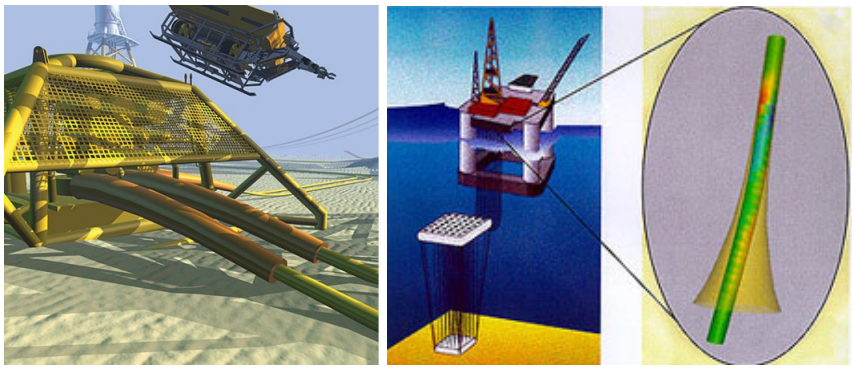

Figure 2.3: End termination

Chapter 3

FAILURE MODES AND DESIGN CRITERIA

3.1 Introduction

A good knowledge and study of pipe failure modes and the relative failure mechanisms is very important in the design process, especially when the water depth increases, namely in the harsh subsea situation. This introduction is mainly based on the Handbook on Design and operation of Flexible Pipes 1992[1]. This chapter includes two parts, and the first part is a general description of pipe performance and possible failure modes, while the second part focuses on the buckling failure modes which is mainly studied in this thesis.

3.2 Failure Modes

3.2.1 Overview

Because of the lake of failure data, the study of failure modes and failure mechanisms for flexible pipes is typically based on the evaluation of pipe structure, function of each layer, interface between pipe and end fitting, materials, pipe properties, operational experience and the relative pipe application. Failure modes will stop the flexible pipe from transporting the fluid from one place to another and sometimes will cause very serious accidents. Considering the properties of flexible pipe, there are only two main failure modes:

- Leakage

- Reduction of internal cross section

The main failures relative to the two main failure modes above is shown in Fig.3.1.

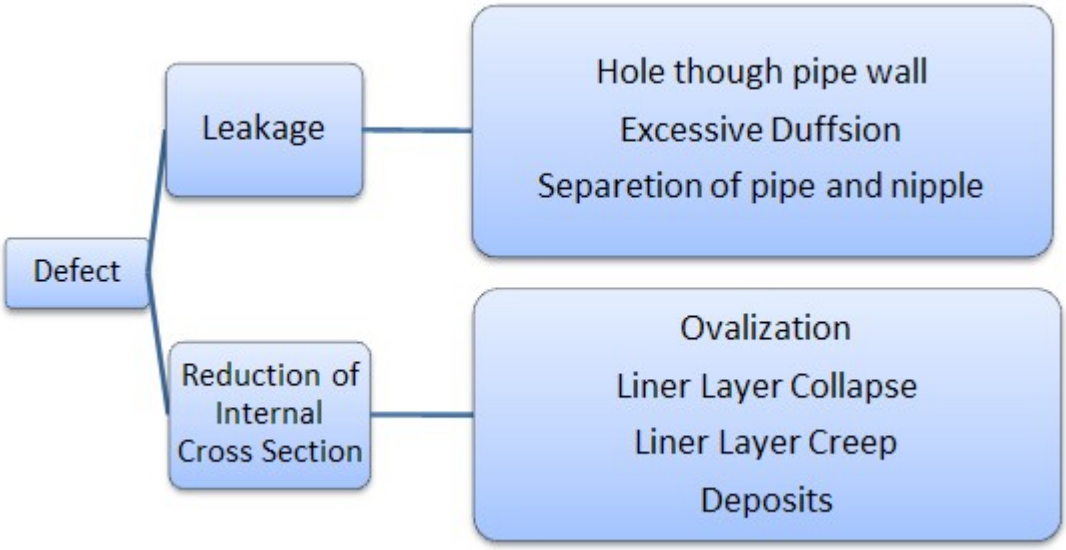

Figure 3.1: The main failures relative to the two main failure modes

The flexible pipe is a composite structure, hence the causes of these failure modes are a combination of many events or partial failures. The initial failure is not enough to cause the full failure, but without regarding of this situation in original design, it will result in further degeneration in service life by other composite failure mechanisms. Table.3.1 illustrates the failure modes and the corresponding failure mechanisms, taken from the Check List of Failure Modes for Primary Structural Design of Unbonded Flexible Pipe in API RECOMMENDED PRACTICE 17B Table[6].

3.2.2 Buckling Failure Modes

The tensile armour failure and the compression failure are more important than other failure modes when the flexible pipe is applied in deep water. These failure modes will lead to tensile armour buckling, so the motivation to study the buckling mechanisms relative to these two modes is to analyse the buckling capacity for design and production. There are two types of tensile armour buckling, namely, the radial buckling and lateral buckling.

Pipe Global Failure Mode	Potential Failure Mechanisms	Design Solution/Variables
Collapse	1. Collapse of carcass and/or pressure armour due to excessive tension. 2. Collapse of carcass and/or pressure armours due to excess external pressure. 3. Collapse of carcass and/or pressure armour due to installation loads or ovalisation due to installation loads. 4. Collapse of internal pressure sheath in smooth bore pipe.	1. Increase thickness of carcass strip, pressure armour or internal pressure sheath (smooth bore collapse). 2. Modify configuration or installation design to reduce loads. 3. Add intermediate leak-proof sheath (smooth bore pipes). 4. Increase the area moment of inertia of carcass or pressure armour
Burst	1. Rupture of pressure armours because of excess internal pressure. 2. Rupture of tensile armours due to excess internal pressure.	1. Modify design, e.g., change lay angle, wire shape, etc. 2. Increase wire thickness or select higher strength material if feasible. 3. Add additional pressure or tensile armour layers
Tensile failure	1. Rupture of tensile armours due to excess tension. 2. Collapse of carcass and/or pressure armours and/or internal pressure sheath due to excess tension. 3. Snagging by fishing trawl board or anchor, causing overbending or tensile failure.	1. Increase wire thickness or select higher strength material if feasible. 2. Modify configuration designs to reduce loads. 3. Add two more armour layers. 4. Bury pipe
Compressive failure	1. Birdcaging of tensile armour wires. 2. Compression leading to upheaval buckling and excess bending.	1. Avoid riser configurations that cause excessive pipe compression. 2. Provide additional support/restraint for tensile armours, such as tape and/or additional or thicker outer sheath.
Overbending	1. Collapse of carcass and/or pressure armour or internal pressure sheath. 2. Rupture of internal pressure sheath. 3. Unlocking of interlocked pressure or tensile armour layer. 4. Crack in outer sheath. SA, DA	1. Modify configuration designs to reduce loads.
Torsional failure	1. Failure of tensile armour wires. 2. Collapse of carcass and/or internal pressure sheath. 3. Birdcaging of tensile armour wires.	1. Modify system design to reduce torsional loads. 2. Modify cross-section design to increase torsional capacity.
Fatigue failure	1. Tensile armour wire fatigue. 2. Pressure armour wire fatigue.	1. Increase wire thickness or select alternative material, so that fatigue stresses are compatible with service life requirements. 2. Modify design to reduce fatigue loads.
Erosion	1. Of internal carcass.	1. Material selection. 2. Increase thickness of carcass. 3. Reduce sand content. 4. Increase MBR.
Corrosion	1. Of internal carcass. 2. Of pressure or tensile armour exposed to seawater, if applicable. 3. Of pressure or tensile armour exposed to diffused product.	1. Material selection. 2. Cathodic protection system design. 3. Increase layer thickness. 4. Add coatings or lubricants

Table 3.1: Check List of Failure Modes for Design of Unbonded Flexible Pipe[6]

Radial Buckling

Radial buckling, the so-called bird-caging buckling, may happen when the anti-buckling tape bears the strength exceeding its ultimate strength, or the elastic buckling happens without tape failure. There will be a sudden tensile armour expansion in radial direction. This kind of failure mode is shown in Fig.3.2 below:

Figure 3.2: Bird-caging[2]

lateral Buckling

Lateral buckling may happen when the anti-buckling tape is strong enough and the tensile armour will only have lateral direction to slide. However, the tensile armour will bear more friction force coming from the neighbour layers and the failure mode is shown in Fig.3.3 below:

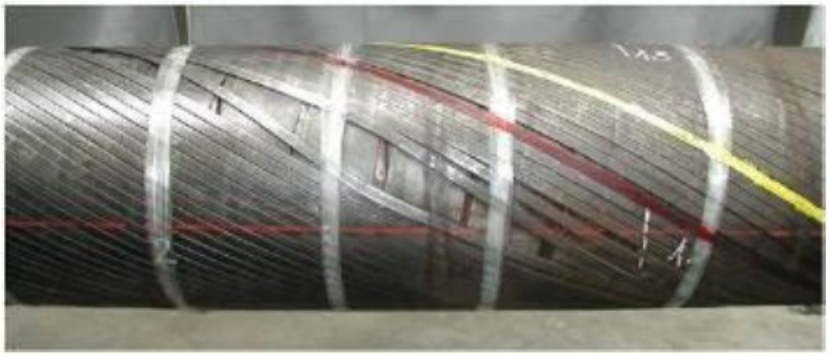

Figure 3.3: Lateral Buckling[2]

The details of the lateral buckling mechanism will be introduced in chapter 4, including

the study of the simplified model by Østergaard and the failure mechanism due to the cyclic bending.

3.3 Design Criteria

This section is according to the API RECOMMENDED PRACTICE 17B[6]. The design criteria for unbounded flexible pipes are given in section 5.3.1 of API Specification 17J[13]:

- a. Strain (polymer sheath).

The allowable strain is the key parameter both in the design of the internal pressure armour and outer sheath. It can be testified by material tests under relevant service and ageing conditions. [6]

- b. Creep (internal pressure sheath).

Under high compression and temperature, the internal thermoplastic sheath will creep into gaps between metal armours until a leakage happens. So it is necessary to decide the maximum allowable reduction of the internal sheath thickness.

- c. Stress (metallic layers and end-fitting).

The allow stress is obtained by providing the acceptable safety factors against failure which decides the maximum stress value. This criteria is very important for flexible pipe design.

- d. Hydrostatic collapse (buckling load).

This criteria is for the bucking load of the internal carcass under hydrostatic pressure. The safety factor for the criteria is the absolute value of the ratio between collapse and design depth, which is so-called collapse to design ratio. The collapse to design ratio will decide whether a sealing intermediate sheath is used to provide more strength to prevent the hydrostatic collapse.

- e. Mechanical collapse (stress induced from armour layers).

It is a design criteria relevant to the internal carcass mechanical collapse due to the excessive tension and should be checked together with the contribution of all supporting steel layers.

- f. Torsion.

There are two different scenarios caused by the two different directions of the torsion acting on the flexible pipe. These two scenarios will decide the maximum torsion factor. One is that the outer tensile armour layer is twisted tight towards the inner tensile armour which gives rise to an increasing pressure between layers. Another is the outer tensile armour layer is twisted outwards the inner tensile armour. The kind of torsion will induce a gap between tensile armour layers. In order to calculate the allowance torsion, the damaging torsion should be used with a safety factor more than 1.0.

- g. Crushing collapse and ovalisation (during installation).

When it comes to the laying operation, which is usually controlled by a laying winch, the pipe will experience the crushing collapse and ovalisation. This will induce an overstressing of the metallic layers and hence it must be controlled to avoid the sudden collapse or significant ovalisation.

There are two limits about the axial tension or radial compression and the effective tension or radial compression must be considered to decide the design maximum criteria. And the maximum permanent ovalisation should be taken account into.

- h. Compression (axial and effective).

Compression is the cause of pipe buckling and deformation, and it includes two compression types: one is the effective compression inducing an increasing deformation of pipe, and the other is the axial compression causing the bird-caging buckling in the tensile armour.

According to the document (API RECOMMENDED PRACTICE 17B), if the effective compression occurs, it should satisfy two limits, “a. The effective compression should be less than that which would cause the MBR criteria to be violated. b. Bar buckling of the pipe should not occur”.[6]

If the axial compression occurs, “The maximum axial compression for an unbounded flexible pipe should be calculated as the value which causes a gap between the tensile armour wires and the underlying layer equal to half the thickness of the armour wire”.[6]

The checking process of these two compression types should be carried out in the design process.

- i. Service life factors.

In order to decide the service life of pipe, the two important factors known as fatigue life(can be obtained from fatigue calculation) and the permissible levels of degradation, need to be checked.

Chapter 4

THEORY AND ANALYTICAL METHOD

4.1 Introduction

This chapter is to introduce the theory background of this thesis, and there is no need to include all the details but the one hitting the points of the topic. In this chapter, a brief introduction of the finite element method including the non-linear finite element method is presented. A description and the related theory background of the element used in the analysis of transverse buckling is given as well as a overview of the FEM software Bflex2010 and Marc. The analytical solution of the transverse tensile armour buckling load is introduced at the end of this chapter.

4.2 Non-linear Finite Element Methods

4.2.1 Introduction

In order to solve the complicated problems related to the structures and continua, the finite element method is used to get the exact results by the computer program. Finite element method was developed with the fast improvement of the computer technology, resulting in the high speed and efficient approach to solve the engineering problems, such as the design of building, aircraft, ship and offshore structures, the analysis of the buckling, collision, fatigue and fracture problems. This section is a general introduction of the finite element method and

non-linear finite element method.

4.2.2 Finite Element Method

The basic principle of finite element method is to discretize the structure into a finite number of elements, then analyse and integrate all the elements to carry out the global or local analysis. Each element contains a number of nodes and the mechanics behaviour is determined by the nodal displacements independently. In order to decide the nodal displacement, the displacement pattern should be decided and usually assumed as linear, quadratic, or cubic, corresponding to the higher order interpolation function to increase the accuracy rate. The finite element method relative to the structural mechanics is based on three principles[14]:

- 1. Equilibrium

For each element, the stress components must be balanced with the body forces, which is in general described by:

$$\Delta^T \cdot \boldsymbol{\sigma} + \mathbf{f} = \mathbf{0} \tag{4.1}$$

where $\boldsymbol{\sigma}$ is the stress components and $\mathbf{f}$ is the volume forces.

- 2. Compatibility: Strain-displacement relationship

In finite element method, the relationship between strain and displacement should be decided and for example the 2D strain-displacement relationship is:

$$\boldsymbol{\varepsilon} = \Delta \cdot \mathbf{u} \tag{4.2}$$

where the strain vector is $\boldsymbol{\varepsilon} = \begin{bmatrix} \varepsilon_x \\ \varepsilon_y \\ \gamma_{xy} \end{bmatrix}$, the displacement vector is $\mathbf{u} = \begin{bmatrix} u \\ v \end{bmatrix}$, Δ is the differential operator matrix.

- 3. Material law: Stress-strain relationship.

The relationship between stresses and strains is defined in terms of the material law. For linear elasticity problem, the Hook's generalized law is used to describe this. The relationship can be

shown in general as below:

$$\boldsymbol{\sigma} = \mathbf{D} \cdot \boldsymbol{\varepsilon} \tag{4.3}$$

where **D** is the linear elastic transform matrix between stress and strain.

In addition, the boundary condition should be fulfilled by given displacement or stress. If these equations are fulfilled with point by point, the form is called the strong form, however, the finite element method is based on the weak form which lies on the virtual work. With the application of the principle of virtual work, which means that the total potential energy of a system in equilibrium is stationary, the virtual work which is usually related to an integrated equilibrium problem will be used to derive the stiffness relationship.

Step 1 is to establish the element stiffness. The FEM starts with the element discretized from the system and the stiffness of each element is established by the form:

$$\mathbf{S} = \mathbf{kv} + \mathbf{S}^o \tag{4.4}$$

where **S** is the general element nodal point forces, **k** is the element stiffness matrix, **v** is the element displacement vector and the $\mathbf{S^o}$ is the element nodal point force contributing from the distributed loads.

Step 2 is to establish the system stiffness. By assuming the element has the same capacity as the structure, the two forms should be fulfilled:

- Nodal point compatibility (for each element) relationship.

$$\mathbf{v}^e = \mathbf{a}^e \mathbf{r} \tag{4.5}$$

- Nodal point equilibrium (for all nodes): relationship.

$$\mathbf{R}^c + \sum \mathbf{R}^e = \mathbf{0} \tag{4.6}$$

Then the system stiffness can be shown as:

$$\mathbf{R}^c = \mathbf{Kr} + \mathbf{R^o} \tag{4.7}$$

In generally form,

$$\mathbf{Kr} = \mathbf{R} \tag{4.8}$$

$$\mathbf{R} = \mathbf{R}^c - \mathbf{R}^o \tag{4.9}$$

where $\mathbf{K}$ is the system stiffness matrix, $\mathbf{r}$ is the nodal displacement vector, $\mathbf{R}^c$ is the vector of concentrated nodal point forces and $\mathbf{R}^o$ is the vector of element nodal forces. So the relationship between element and system can be derived as:

$$\mathbf{K} = \sum_{e=1}^{n_e} \mathbf{K}^e = \sum_{e=1}^{n_e} (\mathbf{a}^e)^T \mathbf{k}^e \mathbf{a}^e \tag{4.10}$$

Here $\mathbf{a}^e$ is the so-called connectivity matrix and $\mathbf{R^o}$ is found from the form:

$$\mathbf{R^o} = \sum_{e=1}^{n_e} (\mathbf{a}^e)^T \mathbf{S}^{oe} \tag{4.11}$$

Step 3 is to include the boundary Conditions. The prescribed boundary conditions are added into by suppressing restrained nodal displacements. Then the stresses resultants can be computed from nodal point displacements.

4.2.3 Non-linear Finite Element Method

Tensile armour buckling problem is a nonlinear problem, hence a non-linear finite element method must be carried out to solve this kind of problem.

In the analysis of linear finite element method, it is based on two assumptions, that is, the displacement is small and the material is linear and elastic. However, when it comes to the calculation of the ultimate strength for the buckling and collapse problems, the significant change of geometry should be considered and the material will not be elastic and linear due to the large structural deformation. For this kind of problem, the non-linear finite element method is necessary to be carried out.

For the analysis of flexible pipe, the non-linear finite element method is applied to calculate the complex mechanism behaviours, especially for the contact and buckling problems.

As it is illustrated above, the source of nonlinearities relative to the flexible pipe includes:[3]

- Large displacements (geometrical nonlinearity)
- Non-linear material behaviour

- Non-linear pipe-soil interaction forces
- Non-linear hydrodynamic loading
- Variable boundary conditions
- Transient temperature and pressure loads due to variable fluid flow conditions

The key to carry out the non-linear finite element method is to solve the nonlinear equation which takes account a second order effect into. The nonlinear equation is solved by an incremental procedure. For each load increment, an equilibrium iteration is carried out, and the method which is known as the Newton-Raphson Iteration loop is widely used in the FEM software, such as Bflex.

The main solution procedure of Newton-Raphson Iteration loop is:

1. Build the global tangential stiffness matrix $\mathbf{K}_T$ and load increment $\Delta\mathbf{R}$

The first step is to build the element stiffness matrix $\mathbf{k}_{Ti}$ and to calculate the element load vector in this form $\Delta\mathbf{S}_i = \mathbf{S}_i^{ext}(t+\Delta t) - \mathbf{S}_i^{int}(t)$. Then the stiffness matrix and element load vector are transformed into a global system transformation matrix $\Delta\mathbf{T}_i$ by the formula $\mathbf{T}_i^T\mathbf{k}_{Ti}\mathbf{T}_i$ and $\mathbf{T}_i\Delta\mathbf{S}^i$. The last step is to add the transformed stiffness $\mathbf{k}_{Ti}$ and $\Delta\mathbf{S}^i$ to the global tangential stiffness matrix $\mathbf{K}_T$ and load increment and $\Delta\mathbf{R}$.

2. Solve the linear equation system $\mathbf{K}_T\Delta\mathbf{r} = \Delta\mathbf{R}$,$\Delta\mathbf{r}$ is the change of nodal displacement vector and is derived by the formula:

$$\Delta\mathbf{r} = \mathbf{r}^{i+1} - \mathbf{r}^i = -\frac{\mathbf{g}(\mathbf{r})}{\frac{\partial\mathbf{g}}{\partial\boldsymbol{r}}} \tag{4.12}$$

where i is the iteration number.

3. Update the nodal and element quantities and compute the convergence rate to decide whether to continue the iteration.

There are two kinds of problems in the nonlinear analysis of marine structure, namely, the static analysis and the dynamic analysis. The static analysis can be solved by modal superposition while the dynamic analysis can be solved by the direct time integration of the motion equation. And the Newton-Raphson Iteration is performed as the equilibrium iterations which is the same between the two kinds of analysis.

4.3 Non-linear FEM Code

This section is a general introduction to the computer program relative to the nonlinear element method code. The FEM software Bflex2010 and Marc are given a brief overview and the theory background related to the established model in Bflex2010 is introduced in details.

4.3.1 Bflex

Bflex is the finite element method computer program which is developed by SINTEF Marintek. Blfex2010 is the newest version of Bflex for the global analysis and stress analysis of the tensile armour layers. Bflex is based on the principle of virtual displacement and the Co-rotational Total Lagrangian formulation as the non-linear finite element formulation is applied in software which covering the non-linear effect. In the analysis of tendons bending, the Loxodromic curve elastic bending theory is used which neglecting the transverse slip based on the work by Sævik.

The non-linear element method used in Bflex is the same to the procedure illustrated above, which applying the Newton-Raphson Iteration method to carry out the non-linear FEA.

4.3.2 Marc

Marc is the FEA software developed by the MSC Software. Marc is a general-purpose, nonlinear finite element analysis solution to accurately simulate the response of the products under static, dynamic and multi-physics loading situations. Marc is a functional software with the advantage in modeling the nonlinear material behaviors and transient environmental conditions to solve the complex design problems. It can perform the linear and nonlinear stress analysis in the static and dynamic regimes. The nonlinearities may be due to either material behavior, large deformation, or boundary conditions as illustrated above and Marc can give the accurate representation of the nonlinearity.

The structure of Marc contains comprehensive libraries, structural procedures, materials, elements, and program functions and with the combination of these libraries, Marc can deal with many real engineer problems.

For the nonlinear element method in Marc, the total Lagrangian procedure is used. When it comes to the large deformation problem that the nonlinear terms in curvature expression

cannot be neglected and, an update total Lagrangian procedure is applied. In the procedure, displacement-based elements is used which will be more efficient, and Cauchy stress (true stress) and logarithmic strain are applied with Updated Lagrange formulation.

The procedure to perform the equilibrium iterations is the same to Bflex, namely, the Newton-Raphson Iteration. But in Marc, there are different methods for the different scenarios. For large-scale nonlinear problem, a Modified Newton-Raphson Method will be used without re-assembling the stiffness matrix in each iteration. When the rotations are large, but membrane stresses are small, a strain correction method is used to make the process simple and effective by applying a linearized strain calculation.

4.3.3 Theory Background in Bflex2010

Element Description

There four types of element applied in the models established in Bflex2010. The simplified model includes one layer named core to present the supporting layer against the tensile layer and one tendon rolling on the core to present the tensile layer. Element PIPE31 is used to build supporting layer and element HSHEAR353 is used to build the tensile layer.

The full model includes all layers and anti-buckling layer, and element HSHEAR363 is used to build the structural tape, the anti-buckling tape and sheath. In addition, element HCONT463 is applied to present the contact layers between the physical layers. This section is mainly based on the Bflex2010 theory manual[11] and the Svein Sævik's PhD thesis[15].

Pipe Element

The pipe element in Bflex2010 is the finite element model including six beam degrees of freedom per node. The motion and orientation of the beam node refers to a global coordinate system with base vectors $\mathbf{I}_i$. However, the element deformation is measured referring to a local beam element system $\mathbf{j}_i$ tied with each element. Figure.4.1 shows the definition of the motion of beam nodes.

The contribution to the equilibrium equation from beam is based on the assumption that the Bernoulli-Euler and Navier hypothesis are applied. To formulate the incremental equilib-

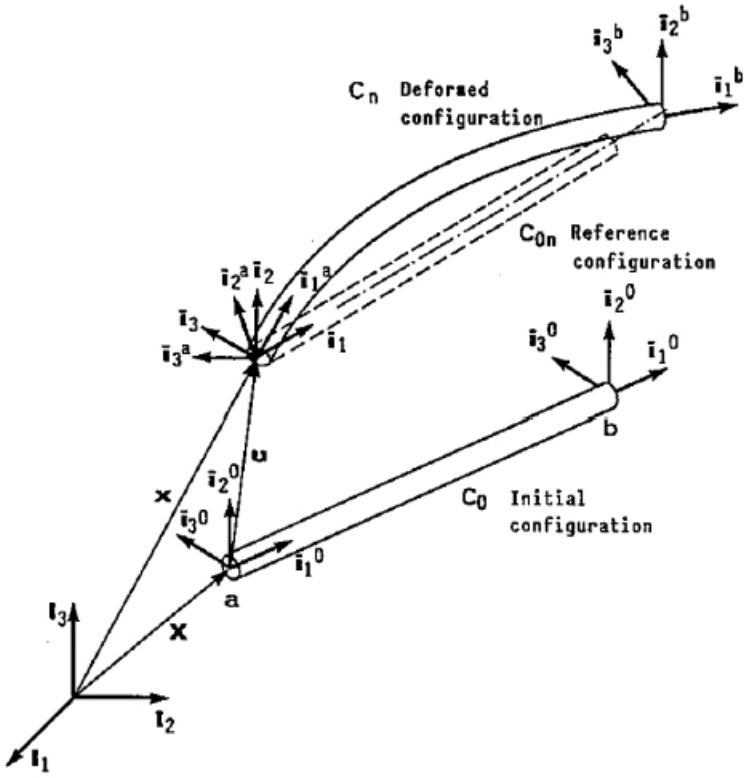

Figure 4.1: Motion of beam nodes

rium equations, Green strain tensor is applied as the measurement of strain. The pipe element used in model is PIPE31, the elastic beam element, which means the second order longitudinal strain term in the Green strain tensor as well as the coupling terms between longitudinal strain and torsion are neglected and the same to the shear deformation.

The longitudinal Green strain is:

$$E_{xx} = u_{x_0,x} - y u_{y_0,xx} - z u_{z_0,xx} + \frac{1}{2}(u_{y_0,x}^2 + u_{z_0,x}^2) \tag{4.13}$$

where the displacements of an arbitrary point P can be defined by the expression of local coordinates x, y, z.

$$\begin{cases} u_x = u_{x_0} - y u_{y_0,x} - z u_{z_0,x} \\ u_y = u_{y_0} - z\theta_x \\ u_y = u_{z_0} - y\theta_x \end{cases} \tag{4.14}$$

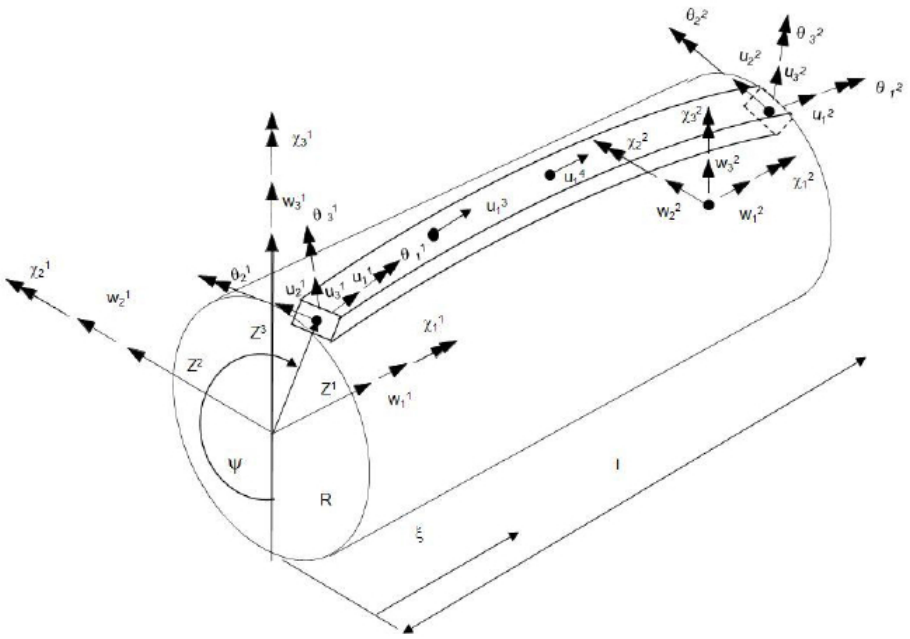

Figure 4.2: The Dofs of HSHEAR353

Helix Shear Element

The helix shear element(HSHEAR) is used to establish the tendon in the tensile layer. The standard beam element usually insists two nodes with six degrees of freedom. However, in Bflex2010, the HSHEAR353 element includes two additional nodes to describe the motion as a sum of standard beam quantities. So it is possible to describe the condition that the plane surfaces remain plane and to compute the relative deformations when the slide happens.

There are 24 degrees of freedom in the HSHEAR353 element, including 12 Dofs from the standard beam on the centreline to describe the prescribed global strain quantities and the other 12 Dofs are used to describe the local displacement of the wire relevant to the core. This element will ensure the cubic interpolation in all directions to avoid the membrane locking phenomena due to the curvature coupling terms.

The degrees of freedom of HSHEAR353 is shown in the Fig.4.2.

In order to describe the kinematic quantities of relative deformation, some assumptions should be introduced. If the shear deformations including the end sectional warp are ignored and only the motion of the helix centre line is considered, the kinematic quantities which deciding the longitudinal strain can be obtained. It was formulated by Svein Sævik in 1993[16] and

2011[17].

$$G_m E_{11} = \epsilon_1 + X^3\omega_2 - X^2\omega_3 + \frac{1}{2}\epsilon_1^2 + \frac{1}{2}\epsilon_2^2 + \frac{1}{2}\epsilon_3^2 \tag{4.15}$$

where:

$$\epsilon_1 = u_{1,1} - \kappa_3 u_2 + \kappa_2 u_3 \tag{4.16}$$

$$\epsilon_2 = u_{2,1} + \kappa_3 u_1 - \kappa_1 u_3 \tag{4.17}$$

$$\epsilon_3 = u_{3,1} - \kappa_2 u_1 + \kappa_1 u_2 \tag{4.18}$$

$$\omega_1 = \kappa_1 u_{1,1} - \kappa_t u_{2,1} + \kappa_3(u_{3,1} + \kappa_1 u_2) + \kappa_2(u_{2,1} - \kappa_1 u_3) + \omega_{1p} \tag{4.19}$$

$$\omega_2 = -u_{3,11} + \kappa_2 u_{1,1} - 2\kappa_1 u_{2,1} - \kappa_3\kappa_t u_2 + \kappa_1\kappa_1 u_3 + \omega_{2p} \tag{4.20}$$

$$\omega_3 = u_{2,11} + \kappa_3 u_{1,1} - 2\kappa_1 u_{3,1} + \kappa_2\kappa_t u_2 - \kappa_1\kappa_1 u_2 + \omega_{3p} \tag{4.21}$$

The definition of the kinematic quantities and coordinate system is shown in Fig.4.3.

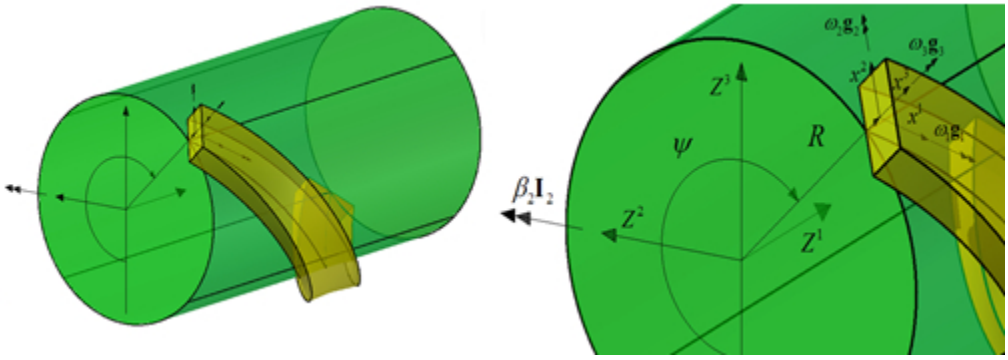

Figure 4.3: The definition of the kinematic quantities and coordinate system

$u_{i,j}$ is the differentiation of the displacement components u_i along the axis X_i with respect to the curve linear coordinate X_j. E_{11} is the Green strain tensor in curve linear coordinates, and G_m is the metric. ϵ_1 represents the 1st order axial strain, ϵ_2 is the centre line rotation about the X_3 axis, and ϵ_3 is the centre line rotation about the X_2 axis.

ω_1 is the torsion of the centre line ,ω_2 and ω_3 are the curvatures about the X_2 and X_3 axis respectively. The ω_{ip} represents the prescribed torsion and curvature quantities from bending while the the initial torsion and curvatures is represented by κ_i.

The HSHEAR363 element is used to establish the structural tape and the anti-buckling tape. This sort of element is different from the standard beam element. The HSHEAR363 includes one

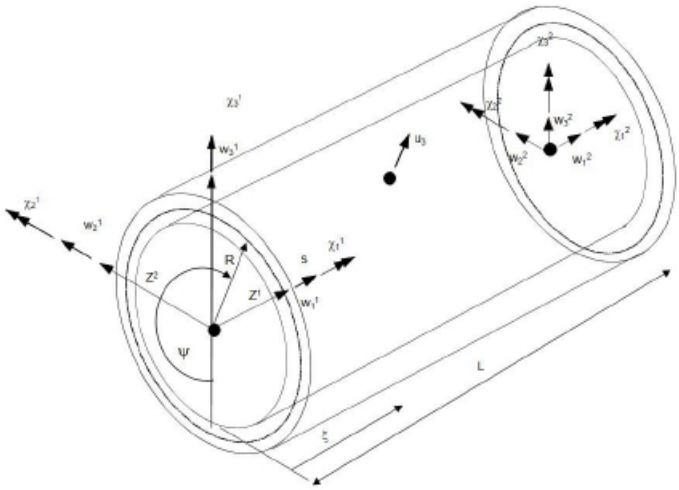

Figure 4.4: The Dofs of the element HSHEAR363

additional node to capture the radial motion by the local radial and ovalization motions. This element can be treated as a simplified shell element making it possible to model different layers in the similar way, which may include the pressure armour, structural tape, anti-buckling tape, the isolation layer and outer sheath.

There are 15 degrees of freedom, including 12 dofs in two standard beam nodes and 3 additional dofs in the extra node in the middle of the element. The additional dofs are introduced to describe the circumferential strain and the associated ovalization. The dofs of the element HSHEAR363 is shown in Fig.4.4.

The reason to introduce this element is to character the plastic layer, the pressure armour, the structural tape and anti-buckling tape. For the plastic layer, the strain quantities are:

$$\varepsilon_{11} = \omega_{1,1} + \omega_{3,11} R\cos\psi - \omega_{2,11} R\sin\psi \tag{4.22}$$

$$\varepsilon_{22} = \frac{u_3}{R} - u_{3,22} X^3 \tag{4.23}$$

$$\varepsilon_{12} = R\chi_{1,1} \tag{4.24}$$

where index 1 and index 2 refer to the Z^1 axis and X^2 axis.

For the pressure armour and tape layer, the longitudinal strain is shown as the formula be-

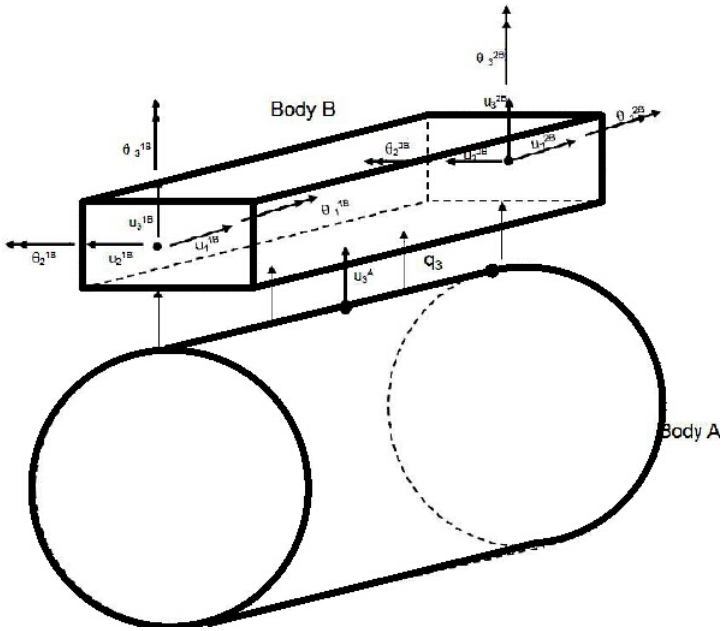

Figure 4.5: The Dofs of the curved contact element

low.

$$\varepsilon_{11} = \cos^2\alpha\omega_{1,1} + \frac{\sin^2\alpha}{R}u_3 + R\sin\alpha\cos\alpha\chi_{1,1} - u_{3,22}\sin^2\alpha X^3 \tag{4.25}$$

Helix Contact Element

The contact element used between the structural tape and the tensile armour is HCONT463, which is the helix contact element developed to fit the beam elements HSHEAR353 and HSHEAR363.

If two beam elements A and B which are shown in Fig.4.5 are taken into account, two general contact conditions may happen after a time increment Δt :

1. Gap opening

$$g = (\Delta\mathbf{u}_B - \Delta\mathbf{u}_A)\cdot\mathbf{n} + g_0 \geq 0 \tag{4.26}$$

2. Contact

$$g = (\Delta\mathbf{u}_B - \Delta\mathbf{u}_A)\cdot\mathbf{n} + g_0 < 0 \tag{4.27}$$

where g is the current gap at the time $t + \Delta t$ in the direction $\mathbf{n}$

As for the element HCONT463, the contact kinematics can be expressed as below:

$$\Delta u_n = (\Delta \mathbf{u}_B - \Delta \mathbf{u}_A) \cdot \mathbf{n} = (\Delta u_3^{0B} - \Delta u_3^{0A}) \tag{4.28}$$

where $\Delta \mathbf{u}$ is an increment in displacement associated to an time interval $[t, t + \Delta t]$, $\mathbf{n}$ is the outward surface normal vector of body A.

The contact element includes three nodes, connecting two end nodes from the element HSHEAR353 and one node from the element HSHEAR363, to describe the longitudinal displacement in X_1 direction and the transverse displacements in X_2 and X_3 directions in HSHEAR 333 altogether with the radial displacement in HSHEAR363. Since the helix contact element is made up with the nodes from element HSHEAR353 and HSHEAR363, the degrees of freedom is also the sum of the chosen Dofs of these two elements. The displacements along the helix beam HSHEAR353 side includes the axial, transverse and radial displacement and is described by 10 DOFs whereas the HSHEAR363 side includes 3 DOFs which gives 13 DOFs in total in the contact element.

4.4 Analytical Methods for Stress and Buckling Analysis in Tensile Armour

4.4.1 Definition of Stress Components in Tensile Armour

The stress state in tensile armour is 3D, as well as other layers in flexible pipe. As the tensile armour provides most of the structural strength and is consisted of many long slender helical beams, the longitudinal stress will be the primary stress in the strength analysis. The stresses are result in two kinds of load scenario. One is the axisymmetric loads, including tension, torsion, internal and external pressure loads, and another is bending.

Firstly, the coordinate definition of the general stress components is given as Fig.4.6[3].

The general stress components contain three normal stress components $\sigma_{11}, \sigma_{22}, \sigma_{33}$, and three shear stress components $\sigma_{12}, \sigma_{23}, \sigma_{13}$

Secondly, the coordinate definition of initial torsion and curvature and the corresponding

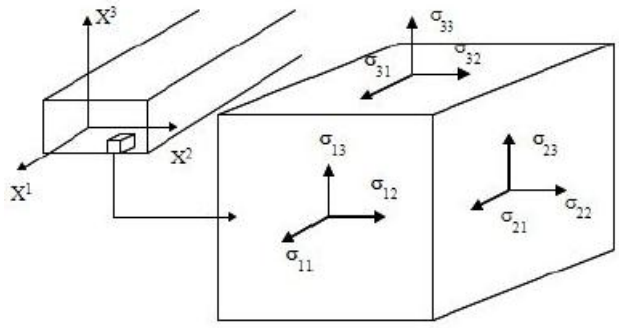

Figure 4.6: General stress components

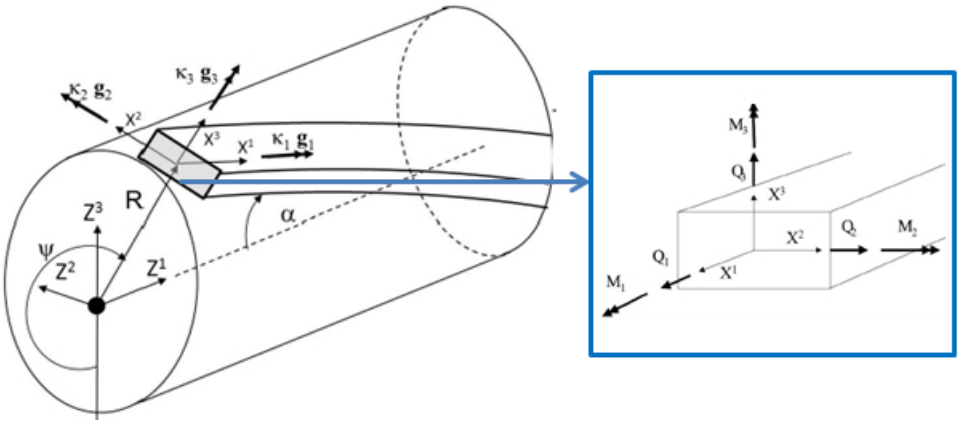

Figure 4.7: Initial torsion and curvature and wire stress resultants[3]

wire stress resultants are shown in Fig.4.7.

Where κ_1 is the initial torsion, κ_2 is the normal curvature, and κ_3 is the transverse curvature. These curvatures are about cross-section axis. In the axisymmetric model, the strain field has to be constant based on the assumption of cylindrical deformation (cylindrical shape is kept during deformation) which resulting in κ_3 is zero.[17]

Basing on the definition above, the significant stress components in the tensile layer are represented in Fig 4.8.[3]

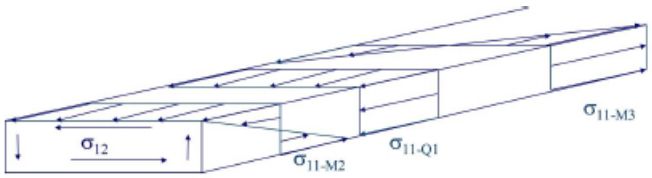

Figure 4.8: Stress components in tensile armour

The components of shear stresses $\sigma_{12}, \sigma_{23}, \sigma_{13}$ is the results stress from the local shear forces Q_1, Q_2, Q_3, in addition, the Q_2 and Q_3 is normally small and can be neglected.

4.4.2 Analytical Method for Stress in Axial Loading Problem

In general, the behaviour relative to axil load is based on the assumption that the cylindrical shape will be the same during deformation, which means the analysis will not consider the collapse or buckling effect. As the definitions illustrated above, the initial torsion and normal curvature can be expressed by the tensile layer radial R and lay angle α. The tensile wire can be described by the curve beam theory.[3]

$$\kappa_1 = \frac{\sin\alpha\cos\alpha}{R} \tag{4.29}$$

$$\kappa_2 = \frac{\sin^2\alpha}{R} \tag{4.30}$$

$$\kappa_3 = 0 \tag{4.31}$$

There are six differential equations used in curve beam theory to describe the equilibrium of the tendon. With the assumption of cylindrical deformation, the strain field has to be constant and all the terms with regard to κ_3 is zero. So there only two differential equations left:

$$-\kappa_2 Q_1 + \kappa_1 Q_2 + q_3 = 0 \tag{4.32}$$

$$-\kappa_2 M_1 + \kappa_1 M_2 + Q_2 = 0 \tag{4.33}$$

The tendon is a slender wire, meaning that the contribution from the bending moment and axil force in transverse direction can be ignored. Thus, the two equations above now become one simplified equation:

$$q_3 = \kappa_2 Q_1 = \frac{\sin^2\alpha}{R} Q_1 \tag{4.34}$$

q_3 is the contact line load in the radial direction. These equilibriums are for the analysis of the behaviour due to the axisymmetric loads, including torsion, tension, internal and external pressure.

For the axial loading problem, the following pure equilibrium for all the metal layers is used

without concerning the effect of the plastic layers.

$$\sum_{j=1}^{N_a} n_j \sigma_{11j} A_j \cos\alpha_j = T_\omega = T_e + \pi p_{int} R_{int}^2 - \pi p_{ext} R_{ext}^2 \tag{4.35}$$

The left side of this equilibrium is the integration of the contributions from different independent layers. A_j is the pipe cross-section area, and α_j is the lay angle of the steel layer, which is different in each layer. σ_{11j} is the axial stress of the layer, and n_j is the number of wires in the layer. For different construction types, there will be a difference in the number of layers and the relative properties. The right hand of the equilibrium is the true wall tension, integrated by the effect tension, contributions from the internal pressure and external pressure.

Normally, the flexible pipe contains two tensile layers and the lay angles are supposed to be equal but opposite in lay direction in order to fulfil the torsion balance. The stresses in the tensile armour can be calculated by this formulation:

$$\sigma_t = \frac{T_\omega}{nA_t \cos\alpha} = \frac{T_w}{2\pi R t_{tot} F_f \cos^2\alpha} \tag{4.36}$$

The t_{tot} is the total thickness for two layers and F_f is the fill factor which defined by the formula:

$$F_f = \frac{nb}{\cos\alpha 2\pi R} \tag{4.37}$$

where b is the width of the tendon, A_t is tensile layer cross-section area and n is the wire number.

4.4.3 The Failure Mechanism and Analytical Method and Model for Lateral Buckling Analysis

The Failure Mechanism

The process of the lateral buckling starts from the result of the end cap force, and the two tensile layers will be squeezed against the anti-buckling tape and a gap will develop between the tensile armour layer and the pressure armour. As the anti-buckling tape is strong enough as the assumption before, the tensile layer only has the longitude direction to slide. The second tensile armour layer will receive the smallest resistant friction force and begin to lose its capacity

first. In order to keep the torsion balance in the cross-section, a loss of the axial compression as compensation is necessary for the first layer which contacting with the anti-buckling tape. Then the pipe will rotate and follow the lay angle direction of the first tensile layer. If the pipe is suffering a cycle loading, a certain rotation will take place during each cycle until the torsion failure criteria of the cross-section reaches.

Analytical Method for Lateral Buckling

If the simplified end is assumed as the boundary condition, the buckling load for the model shown in Fig.4.9 is calculated as the Euler buckling load:

$$P = \frac{\pi^2 EI}{l_e^2} \tag{4.38}$$

where l_e is the buckling length which is influenced by the boundary conditions, which is the length of the bar in this case.

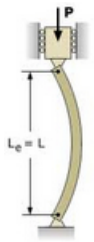

Figure 4.9: Buckling model

For the lateral buckling problem of the flexible pipe, the situation is more complex because the buckling load is mainly carried by the tensile layers, especially the inner layer. If the anti-buckling tape is assumed strong enough and only the inner tensile layer is studied, the tendon in the inner layer only has the lateral direction to go. Under the assumption of no friction, a conservative estimate of the buckling pressure can be achieved from the curve beam differential equation[18]:

$$P = \cos\alpha[\frac{\pi^2 EI_3}{l^2} + GI_1(\kappa_2^2 - \kappa_t\kappa_2) + 4EI_2\kappa_2^1 + EI_3\kappa_2^1] \tag{4.39}$$

where κ_1, κ_2 are the initial torsion and normal curvature and κ_t is the cylinder curvature in

tendon transverse direction, which can be expressed as:

$$\kappa_1 = \frac{\sin\alpha\cos\alpha}{R} \tag{4.40}$$

$$\kappa_2 = \frac{\sin^2\alpha}{R} \tag{4.41}$$

$$\kappa_t = \frac{\cos^2\alpha}{R} \tag{4.42}$$

The inertial moments corresponding to the three axial are listed below, where b is the width of the tendon cross-section and t is the thickness.

$$I_1 = \frac{1}{3}bt^3 \tag{4.43}$$

$$I_2 = \frac{1}{12}bt^3 \tag{4.44}$$

$$I_3 = \frac{1}{12}tb^3 \tag{4.45}$$

where E is the Young's module, and $G = \frac{E}{2(1+\sigma)}$ is the shear module.

In this formulation, as l is very large, the first term will be very small and can be neglected, so the formula can be rewrite to:

$$P = \cos\alpha[GI_1(\kappa_2^2 - \kappa_t\kappa_2) + 4EI_2\kappa_2^1 + EI_3\kappa_2^1] \tag{4.46}$$

It is a function of the tensile layer radial, lay angle and the thickness and width of the tendon cross-section. In general, the fill factor is unchanged for a certain tendon which means the t and b will not change along the buckling analysis of the tensile armour. The buckling pressure function will be reduced as a function of R and α. These parameters are shown in the Fig.4.10:

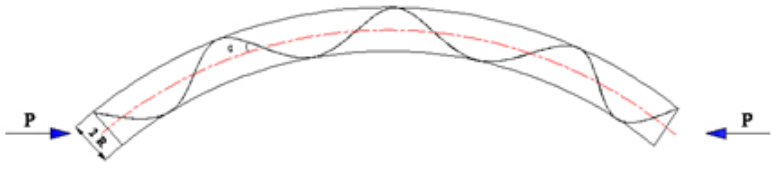

Figure 4.10: Tensile layer radial and lay angle

The basic model in test and the relative strain-force curve are shown as in Fig.4.11:

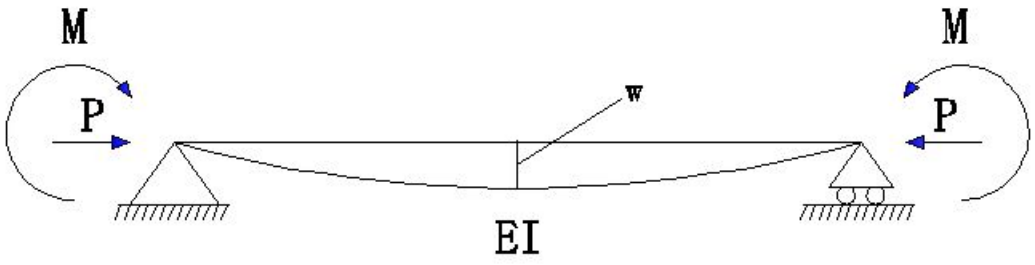

Figure 4.11: Basic buckling model in test

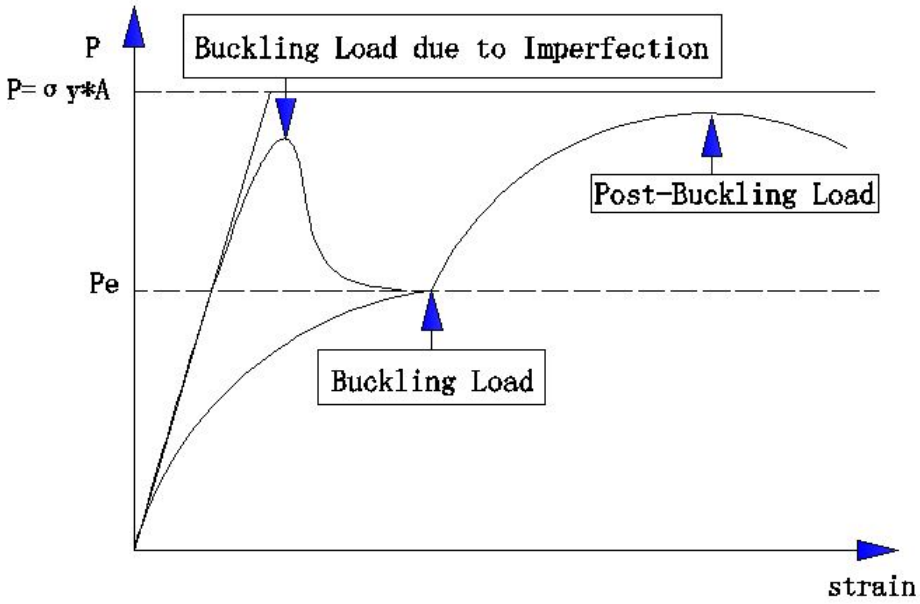

Figure 4.12: Strain-force curve of buckling

Which should be noticed in Fig.4.12 is that the buckling load is divided into two types, one is named as buckling load and another is named as post-buckling load as illustrated in the figure above. The first peak is due to the imperfection in the tendon, which means this part will snap. It should be noticed that the result calculated from the formula is the buckling load. The σ_y is the yield stress, A is the cross-section area and P is the yield load of the tendon.

The post-buckling load happens in the region which is decided by the elastic-plastic behaviour of the material. It is the largest load which the tensile can bear after the buckling happens. So it is necessary to capture both of these loads and study the corresponding behaviours in the test.

Local Model and Global Model of Tensile Armour Layer

The theory was first given by Østergaard in 2012[9], considering a single wire rolling onto the core and bent with a curvature κ. This is modelled by establish a curve on a frictionless toroid as shown in Fig.4.13.[4]

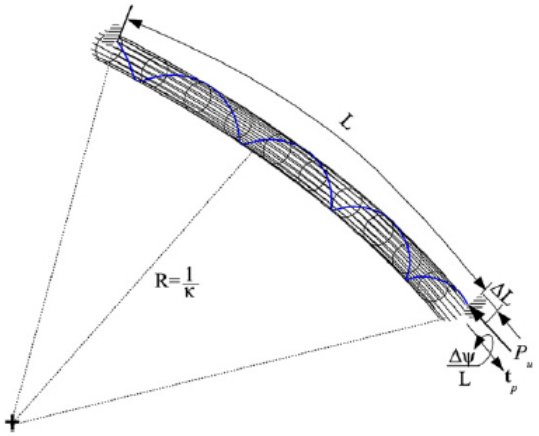

Figure 4.13: Model of armour wire within the wall of a flexible pipe subjected to bending and longitudinal loads[4]

The local model was established based on the toroid with the main radius R and the minor radius r. The two parameters were charactered by two coordinate systems: the arc-length coordinate u along the centreline of the toroid and the circumferential angle coordinate θ. In order to establish the equation system of the wire equilibrium, every point along the toroid was described by a curvilinear coordinate with three orthogonal vectors. The equilibrium was based on the Kirchhoff's equations and the equation system was solved by a Matlab Solver-Boundary Value problem(BVP) solver with the boundary conditions expressed by the pipe strain $\frac{\Delta L}{L}$ and twist rate $\frac{\Delta \Phi}{L}$. Since the outer armour would not suffer the failure mode, the pitch angle of the wire was assumed constant which decreasing the equation order to fourth order to keep the wire equilibrium state in the pipe wall.

The global model is built on the basis of the boundary conditions of the flexible pipe tested in laboratory. The govern equation of the torsional equilibrium was given with the solution based on the Newton-Raphson Iterations steps. After the solution was obtained, the expression of the load carried by the structure was also given.

Chapter 5

BFLEX MODELS

5.1 Introduction

This chapter is an introduction of the model establishment method in Bflex2010, including the simplified model with one tendon and no friction and the full model with all layers. The loading conditions and the correspondingly theoretical and practical background are also introduced, as well as the boundary conditions.

5.2 Simplified Model

The simplified model consists one core and one tensile layer. The core is modelled by element PIPE31 and the tensile layer with 53 tendons is described by one tendon modelled by element HSHEAR353. The friction between the core and the tensile layer is neglected. The length of the model is 6.135m, the inner radial is 0.0985m, and the width of tendon cross-section is 0.01m and the thickness is 0.003m. The layer angle of the tensile wire is 35 degree.

As the tensile layer is represented by one tendon ,a scale factor is used to multiply with the calculated quantities of that tendon. The scale factor is the ratio between total number of helices in one layer and the number of helices used to represent that layer in the model. Another parameter is AXISYM which is for element HSHEAR353, the options are:

- 0 = both interactions are included.

- 1 = turn off axisymmetric shear interaction.
- 2 = turn off bending shear interaction.
- 3 = turn off both axisymmetric and bending interaction.

The simplified model is show in Fig.5.1 below:

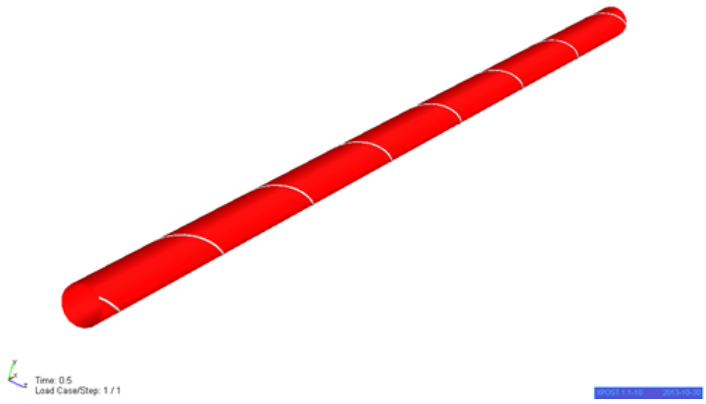

Figure 5.1: Simplified model

Only one core layer and one tendon are built in this model which can be multiplied by a scale factor 53 to represent the effect of the whole tendons in tensile layer. The model is meshed with 200 elements both in the core and tendon. The elements in core are named as 1-200 while the elements in the layer are named as 30001-30200.

5.2.1 Load Condition

The load condition in the model is added as initial element strain. In general, the bending moment and can be computed with the formula:

$$M = EI(\kappa - \kappa_0) \tag{5.1}$$

The formula for axial stress is:

$$\sigma = E\varepsilon = E(\frac{L - L_0}{L_0}) \tag{5.2}$$

Here, the term κ_0 and L_0 represent the initial strain and are put into the Bflex2010, deciding directly the deformation of the shape without any loading condition, such as the concentrated force, distributed load and bending moment.

There are two initial element strain conditions added to the model, one is the axial strain along local X-axis for the first and last element of the tendon with the same value -0.025, and other is the curvature about local Y-axis for the first and last element of the core with the same value -0.0909(1/m).

The analysis of the first 20 seconds is the static analysis, and the next 80 seconds is the dynamic analysis. Firstly, the curvature about local Y-axis is added from 10th second to 20th second, increasing as a ramping function from 0 to -0.0909(1/m). Then the axial strain along local X-axis is added from 20th second to 100th second, increasing as a ramping function from 0 to -0.05(1/m). The ramping function adopted in Bflex2010 is a harmonic function.

5.2.2 Boundary Condition

The boundary condition of the simplified model is introduced below:

- Core: The left end is fixed in five directions expect the curvature along the Y-axis and the right end is fixed only in Z-axis direction.
- Tendon: The left end is fixed in four directions expect the curvature along the Y-axis and Z-axis and the right end is fixed only in X-axis and Y-axis direction.

5.3 Full Model

The full model includes two cores, two tensile layers, one structural tape layer between the two tensile layers, one anti-buckling layer and one sheath layer. One core is modelled by element PIPE31 which is used specially for the loading condition. The other core is used to support the inner tensile layer and is modelled by the element HSHEAR363. The inner and outer tensile layer are built by element HSHEAR353. Each tensile layer is represented by four helix tendons. The structural tape, anti-buckling tape and the sheath are modelled by element HSHEAR363.

The friction between the layers is included and calculated from the contact element which is modelled by element HCONT463.

These four types of element have been introduced in Chapter 4. Since the contact between the anti-buckling tape and the sheath will not influence a lot, the two elements are merged into the same node system, which means there will only be four contact layers for contacting the two tensile layers. Thus the cross section is shown in Fig.5.2. This type of cross section can take the friction and the effect of the contact into account automatically. The friction coefficient between the layers is set to 0.15, which is based on the real flexible pipe structure.

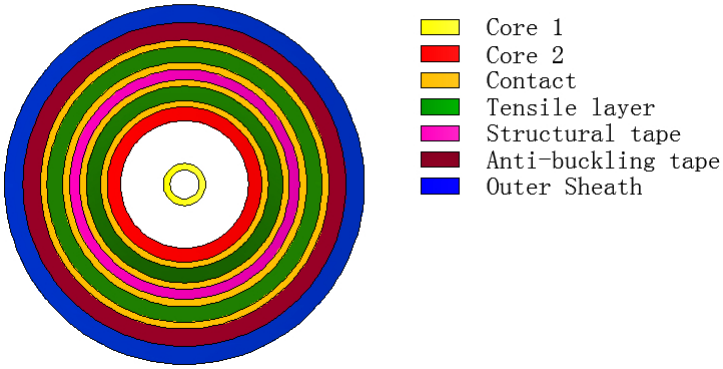

Figure 5.2: Model cross section

Each layer built by element HSHEAR363 is meshed by 100 elements as well as the contact layers. Each tensile layer includes four helix tendon to represent the whole layer and each tendon is modelled by 100 elements, so each tensile layer consists 400 elements. The full model is shown in the Fig.5.3.

The model above is the basic full model and three models were built based on the basic full model with different cross sections: 6 inch riser, 8 inch riser and 14 inch jumper. The parameters of the three models are shown in Tab.5.1[7].

5.3.1 Load Condition

The load condition in the full model is more complex. There are two loading conditions added onto the full model, that is, the bending around the global Y-axis and the compression along the global X-axis.

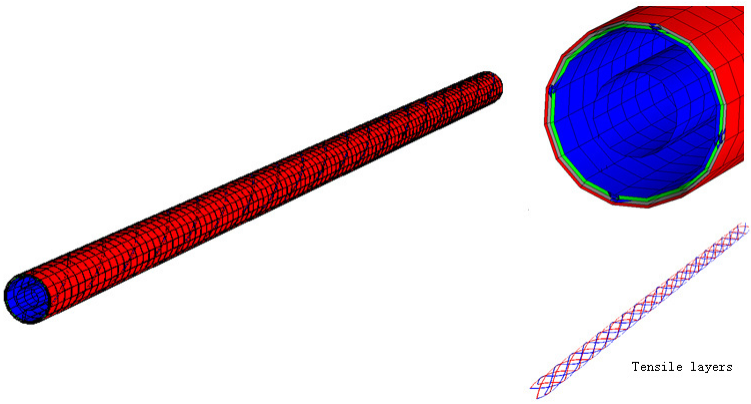

Figure 5.3: Full model

In this section, two models named as "First model" and "Second model" associated with two purposes will be built. In order to study the effects of friction and the anti-buckling tape, one model should be built with the same loading conditions as the simplified model which is named as "First model". However, another full model named "Second model" should be built in another way to study the behaviour of lateral buckling under the cyclic bending.

Bending Condition

As there are many layers in the model, it is not properly to add the initial element curvature to every layer. So the bending is applied by means of the prescribed displacement of the curvature around global Y-axis. The bending condition will be the same for the two models.

Compression Condition

For the compression condition, First model has the same load condition as the simplified model. For Second model, the load condition will be different.

In laboratory, the most common way to add the compression load is to add a pipe with small radius along the central-line in the riser and pull the small pipe to realize the compression acting on the riser. Both ends of the tested riser are fixed with a flange to the Drive housing. This laboratory test system is shown in Fig.5.4[5].

The theory background is shown in Fig.5.5 briefly for clarifying the principles about it. To add tension to the inside small pipe, the pipe will suffer an elongate deformation which is represented by a positive strain. In order to keep the strain balance in the cross section A-A (the

Pipe layer / Pipe Design		6" Riser *1	8" Riser *2	14" Jumper *2
Inner layer of tensile armour wires	Outer diameter (m)	0.201	0.276	0.442
	Pitch length, L_{pitch} (m)	1.263	1.474	2.247
	Pitch angle, φ_{hel} (deg)	26.2	30	31.5
	Wire size (height × width) (mm)	3 × 10	5 × 12.5	4 × 15
	Number of wires	52	54	70
Outer layer of tensile armour wires	Outer diameter (m)	0.209	0.289	0.452
	Pitch length, L_{pitch} (m)	1.318	1.525	2.345
	Pitch angle, φ_{hel} (deg)	-26.2	-30.3	-31.0
	Wire size (height × width) (mm)	3 × 10	5 × 12.5	4 × 15
	Number of wires	54	56	72
High strength anti-birdcaging tape *3	Outer diameter (m)	0.212	0.292	0.455
	Pitch length, L_{pitch} (m)	0.075	0.025	0.140
	Pitch angle, φ_{hel} (deg)	83.5	88.4	-84.4
	Tape size (height × width) (mm)	1 × 60	1.8 × 1.3	1 × 60
	Number of windings	1	8	2
Outer sheath *4	Outer diameter (m)	0.225	0.434	0.477
	Thickness (mm)	6.0	10.0	10.0
	Number of inner layer pitches in pipe sample (including end-fittings)	3.96	3.39	3-34

*1) A basic grade steel used for wires with yield strength of approximately 650 MPa, elastic modulus 210 GPa, Poison's ratio 0.3
*2) A high strength grade steel used for wires with yield strength of approximately 1350 MPa, elastic modulus 210 GPa, Poison's ratio 0.3
*3) Tape material properties chosen are: elastic modulus 27 GPa. Poison's ratio 0.4
*4) Sheath material properties chosen are: elastic modulus 400 MPa, Poison's ratio 0.4

Table 5.1: Pipes design and material properties[7]

sum of strain should be zero), the other layers will suffer a negative strain which can represent the compression behaviour. And the compression will be the same as the tension of the inside small pipe.

The strain balance is shown in the equation 5.3:

$$\varepsilon_{riser} + \varepsilon_{pipe} = 0 \tag{5.3}$$

In Bflex2010, the compression condition is applied in the same way. The small pipe inside the full model in Fig.5.3 is built by element PIPE31, which is a standard beam element with 6 Dofs each node. The material property of this pipe is linear elastic which is under the plane remain plane assumption and subjects to the Hook's law. The positive initial strain(tension) along X-axis is added to the first and the last element of the small pipe, which will result in the compression in all the layers in the riser.

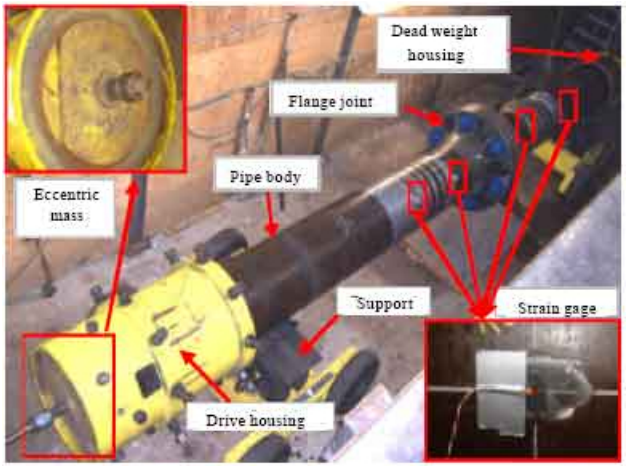

Figure 5.4: Laboratory test rig for compression[5]

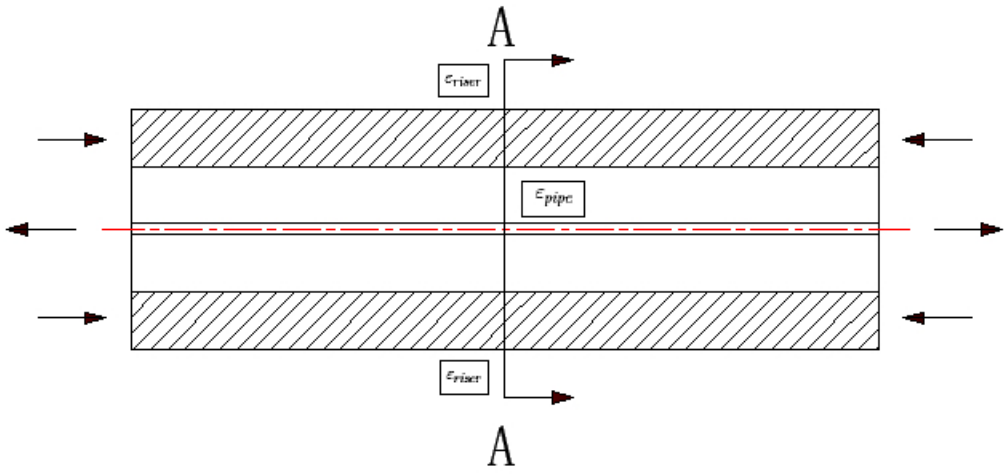

Figure 5.5: Strain balance in cross section A-A

Loading Process

The loading process of First model is the same as the simplified model which has been introduced in the previous section.

However, for Second model, the analysis of the first 10 seconds is the static analysis, and the next 2460 seconds is the dynamic analysis. Firstly, the positive axial strain along local X-axis is added to the small pipe from 0th second to 10th second with one loading step. Then the prescribed curvature around Y-axis is added from 10th second to 2460th second, repeating as a ramping function from zero to the specified curvature based on the data sheet and then back to zero. The ramping function adopted in Bflex2010 is a harmonic function.

Each bending cycle lasts 20 seconds and the time increment is 0.005s in the dynamic analysis, which is very small but necessary to ensure the convergence. However, the program will take very long computing time to finish the calculation.

This loading method is based on the realistic operation behaviour of the riser in the sea. The compression at the two ends of riser is the end-fitting force and the cyclic bending is mainly due to the hydrodynamic load and current.

5.3.2 Boundary Condition

The boundary condition of the First model is the same as the simplified model. However, for the Second model, the boundary condition is dealt with in another way.

The first ten seconds is the static analysis and the purpose of this period is to apply the compression load to the riser, so it will be better to avoid the influence of the other deformations due to the process, which will provide a stable state for the rest dynamic analysis.

Since the small pipe will only suffer a tension load, and to ensure the riser to only suffer a linear stiffness, all the six Dofs of the first node will be fixed, and all the Dofs of the rest nodes along the small pipe will also be fixed except the Dof along the X-axis. This method will allow the whole riser to just bear the compression load without the influence of other relevant deformations. For the two tensile layers, the boundary condition defined in Bflex2010 is the relative displacements in the local coordinate between the element HSHEAR353 and HSHEAR363. So during the first 10 seconds, all the relative displacements will be fixed.

The rest time will be the dynamic analysis and the restart procedure is used, and the purpose of this period is to study the interaction between the tensile layers and the contacted layers during the cyclic bending around Y-axis. Thus only the six Dofs of the first node on the small pipe will be fixed as well as the two Dofs of the last node of the small pipe relative to Y-axis and Z-axis.

For the tensile layers, the relative displacements along and around local Z-axis will be released to capture the behaviour under the cyclic bending.

In addition, the boundary conditions of the rest tape layers are same for both of the two processes. This boundary condition is associate with the three Dofs of the middle node of the element HSHEAR363, which are the two elliptical deformations along the Y-axis and Z-axis and

the hoop deformation. As the riser will suffer a elliptical deformation along the Y-axis, the rest Dofs will be fixed along the pipe.

Chapter 6

BUCKLING PERFORMANCE OF SIMPLIFIED MODEL

6.1 Introduction

This chapter will present the buckling analysis carried out in Bflex2010 and the relative results. The sensitivity analysis will be done to study the time increment, the influence of start process in Bflex2010 and the effect of axisymmetric interaction. A study of the influence of different lay angles will be preformed. In the end, a comparison between the results from Bflex and analytical method will be performed.

In this chapter, six cases based on the simplified model will be preformed for different purposes. Case 1 is to study the common buckling behaviour including the global and local analysis. Case 2 is the study of the the time increment influence. Case 3 and Case 4 are carried out to research the effect of the start procedure and the axisymmetric interaction. The purpose of Case 5 is to study the influence of the lay angle of the tensile armour layer. Case 6 is to research the effect of the cross-section which is relative to the start angle.

6.2 Buckling Analysis of Simplified Model

6.2.1 Global Analysis of Case 1

Case 1. The property of the pipe model used in this case is: the lay angle is 35^o and the start angle is 135^o. After the first 20 seconds, the initial curvature about local Y-axis is added with the time increment 0.01s until the buckling happens. The deformation of the riser during dynamic analysis is shown in the Fig.6.1 below.

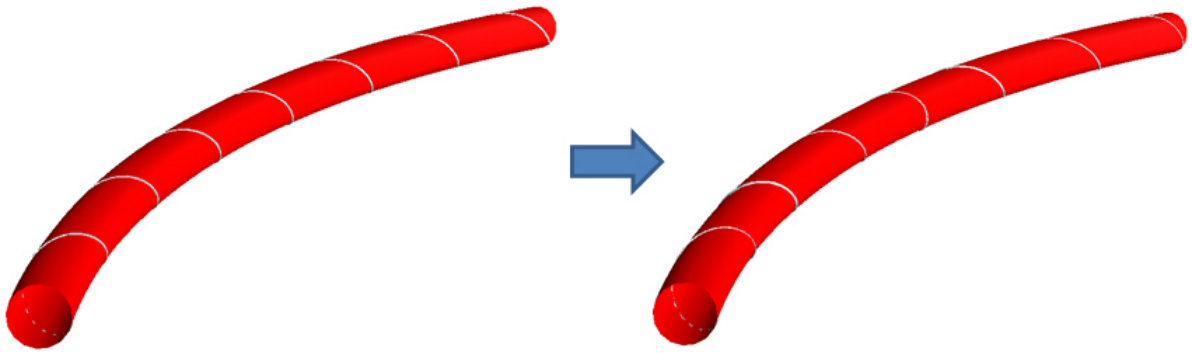

Figure 6.1: Deformation in the static and dynamic analysis , case 1

The global element axial force which is caused by the loading conditions and boundary condition is in general figured in Fig.6.2 below, (plotted by Global Plot in Bflex2010post).

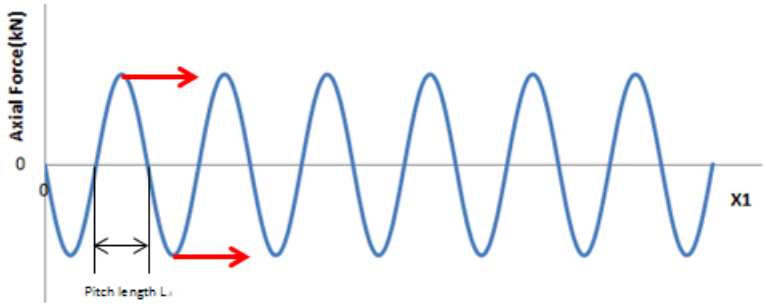

Figure 6.2: Global element axial force of tendon

X1 is the global coordinate in longitude direction along the pipe, the force on the peak or the tough are the points which needs to study because the force is the maximum and the direction is the same as the longitude direction of the riser in this area. So the element in this area should be picked out as the results for buckling study. In case 1, the maximum global element axial force curve at 60th second is shown in Fig.6.3.

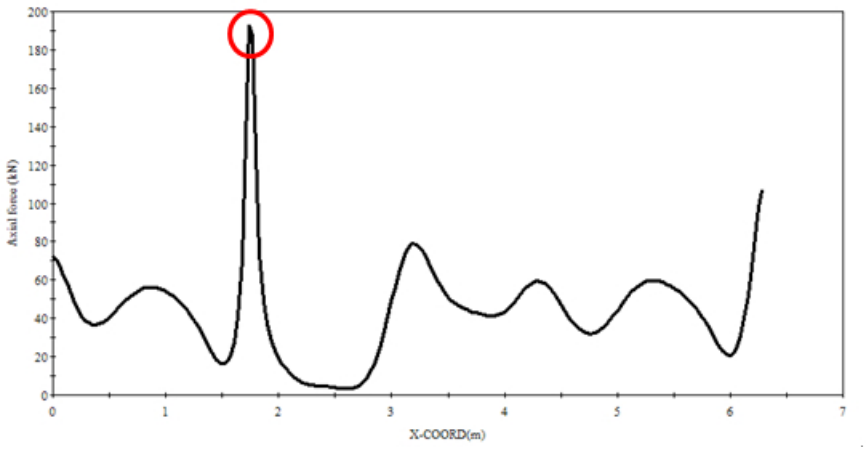

Figure 6.3: Global element axial force curve, case 1

6.2.2 Local Analysis of Case 1

Now the focus is on the position where the buckling happens with the highest stress, and the results in this moment are picked out as in Fig.6.4.

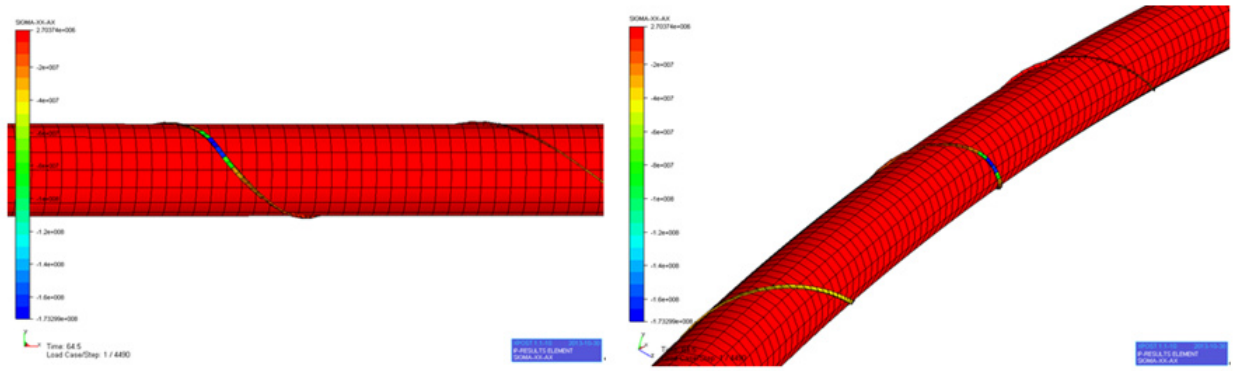

Figure 6.4: Position of buckling(front view and 45 degree view)

In the area where the buckling happens, it is necessary to study and pick out the results of the several elements in this area to decide the maximum buckling force in this area. In this case, the elements with the number 30057, 30058, 30059 with regard to the red circle in global element axial force curve are picked out. For each element in Blfex2010, the definition of the element end number is shown in Fig.6.5.

In our case, the node 3 is picked out and the strain-force curves of these elements are shown in the Fig.6.6. (plotted by Element Plot in Bflex2010post)

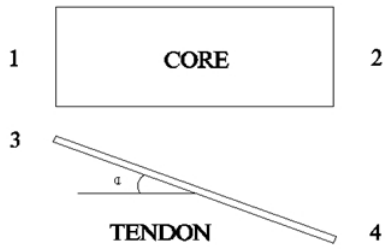

Figure 6.5: Definition of the element end number

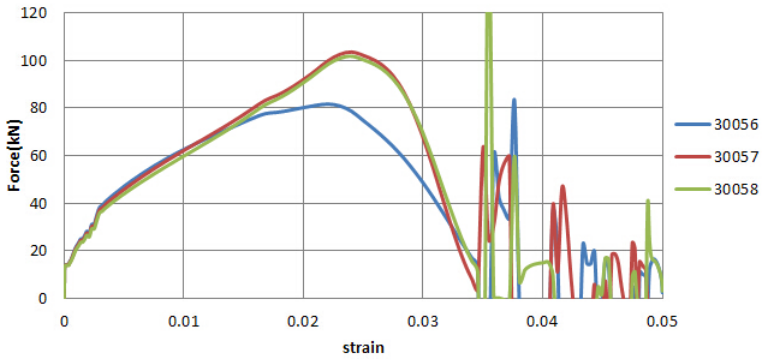

Figure 6.6: Buckling analysis, case 1

The maximum force takes place in the element 30057, and the value is 103.603kN. This value should be multiplied by $\cos(35^o)$ because the force acting on the core is along the global X-axis and the analytical solution is also in this direction. The curve after the strain value 0.035 is chaos, so the results cannot be used to continue the analysis, which means the curve after 0.035 will be cut off. The maximum force value of tendon in global X-axis direction is 84.8611(kN). However, this load is the post buckling load and the buckling load cannot be captured from this test.

The strain-force curve for the core and tendon are both illustrated below to study and testify the reliability of the results in Bflex, and all the force values for tendon should be multiplied by $\cos(35^o)$.

As it is shown in the Fig.6.7, the behaviour before the buckling happens (before the black bar in Fig.6.7) is represented by the linear part of the two curves. As the two curves are almost symmetric to the X-axis, it shows that before the buckling happens, the axial force between the core and tendon are the same in value with opposite direction. This satisfies the equilibrium of the axial force in the system.

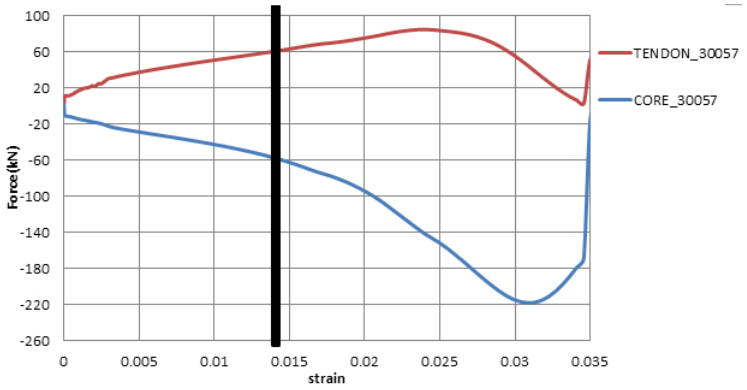

Figure 6.7: Strain-force curve for the core and tendon, case 1

6.3 Sensitivity Analysis

In order to find the influence of the different parameters on the buckling analysis, three sensitivity analyses are carried out. The three parameters are: time increment, axisymmetric interaction and start procedure parameter.

6.3.1 Time Increment

Case 2. Firstly, since case 1 cannot capture the behavior due to the buckling load at the beginning of the buckle, it is necessary to study the influence of the time increment, which is an important parameter in the dynamic procedure both in mathematics and Bflex2010. The time increment in case 1 is 0.01s, but in this case, the time increment is changed to 0.005s. The other conditions are the same as case 1.

The maximum global element axial force curve at 60th second and the results and are shown in Fig.6.9 and Fig.6.8.

The shape is the inverse shape of case 1, the reason may be from the computer procedure. However, as the model in Bflex is a symmetrical model, the locations of buckling of the two cases are equilibrium.

Then the five elements around this area are picked out, the number of the elements is listed in the Fig.6.10 and the strain after 0.025 is chaos and meaningless for the analysis hence that area is omitted and from the figure below, the buckling behaviour at the beginning of buckle can be captured. The peak in the red circle is the influence of the imperfection in the tendon

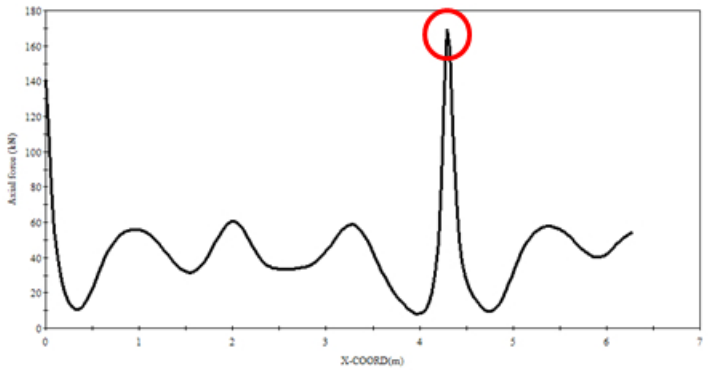

Figure 6.8: Global element axial force curve, case 2

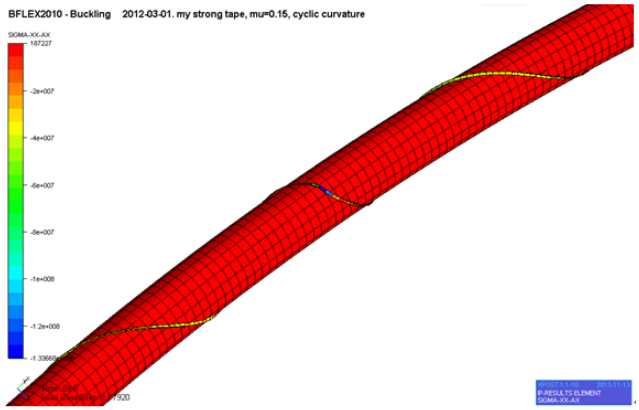

Figure 6.9: Position of buckling (45 degree view), case 2

which can be captured in this case. The imperfection will lead to a sudden increase and the tendon in this position will experience a snap due to it.

It is necessary to compare the results with that from case 1 which is shown in Fig.6.11.

The curve of case 1(blue line) cannot capture the buckling behaviour at the beginning, which is the imperfection behaviour. The maximum force is bigger than the curve of case 2(red line), which means the results of case 1 is not exact and overestimate the maximum force which will lead to a serious problem in the real practical issues.

In order to testify the reliability of the results, the linear test of the core and tendon should be carried out as the same procedure in case 1. The results are shown in Fig.6.12. The linear part is exactly the same which testifies the reliability of the results. As a result of the accuracy, the parameter of case 2, namely, the 0.001s time increment, will be selected as the new time increment condition in the following sensitivity analysis. The results of case 2 will be used as

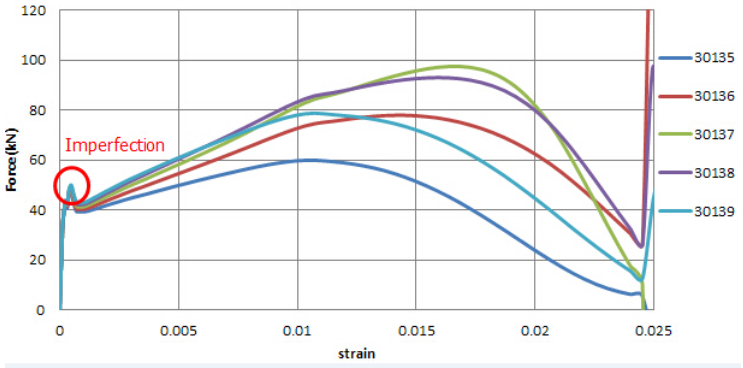

Figure 6.10: Buckling analysis for case 2

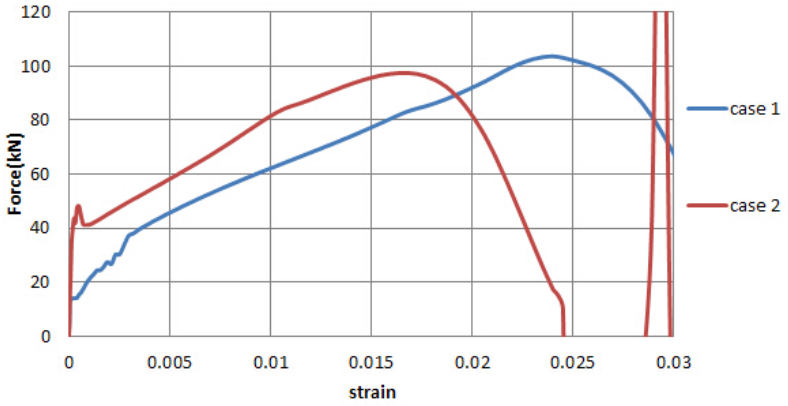

Figure 6.11: Comparison between case 1 and case 2

the results for comparison in the following cases.

6.3.2 Axisymmetric Interaction

This part is force on the influence of the axisymmetric interaction which is represented in Bflex2010 as four optional parameters:

- 0 = both interactions are included.
- 1 = turn off axisymmetric shear
- 2 = turn off bending shear interaction.
- 3 = turn off both axisymmetric and bending interaction.

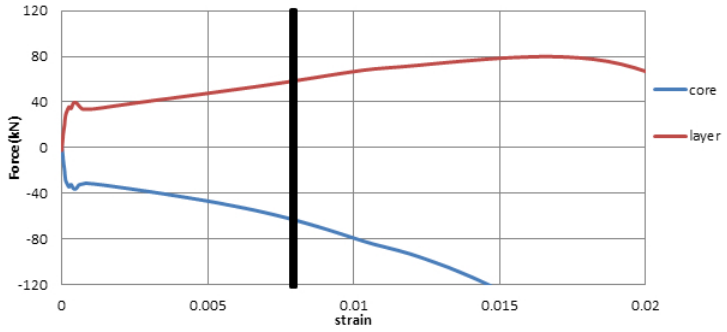

Figure 6.12: Strain-force curve for the core and tendon, case 2

In Bflex2010, the option 1 means there will no shear interaction between the core and tendon. The option 2 means no bending shear interaction will transmit from the core to the tendon. In both case 1 and case 2, the option is set as 0.

Case 3. The analysis will be carried out under the option 1. The procedure is the same as case 2. The time increment is 0.001s. As there is no shear interaction between the core and tendon, the Global element axial force will be zero and the force in core will also be zero.

So there is only one way to figure out the maximum force, that is, to get all the force-strain curves of all the elements and pick out the maximum one and except the elements near the two boundaries.

In the Fig.6.13, the results of the maximum forces are almost the same between the two cases and result in case 3 is slightly larger than case 2.

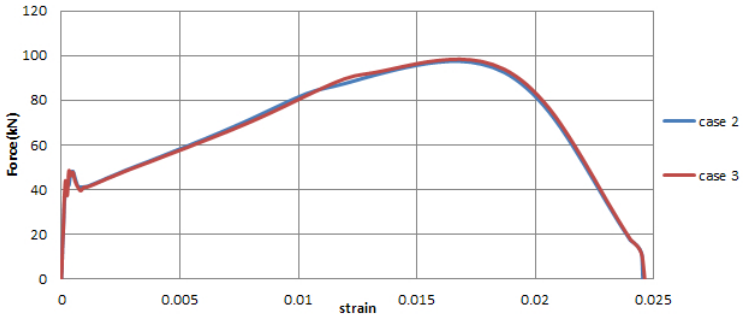

Figure 6.13: Comparison between case 2 and case 3

6.3.3 Stress Free and Restart Procedure

In Bflex2010, the start procedure parameter includes two types:

- Stress free which means that the initial configuration is stress free.
- Restart which means the procedure will restart from previous analysis.

Case 4. The analysis will be carried out under the Restart procedure. And the time increment and the analysis process are the same as case 2. The comparison results are shown in Fig.6.14. From the figure, the value of the maximum force in case 4 is a little smaller than case 2. And the

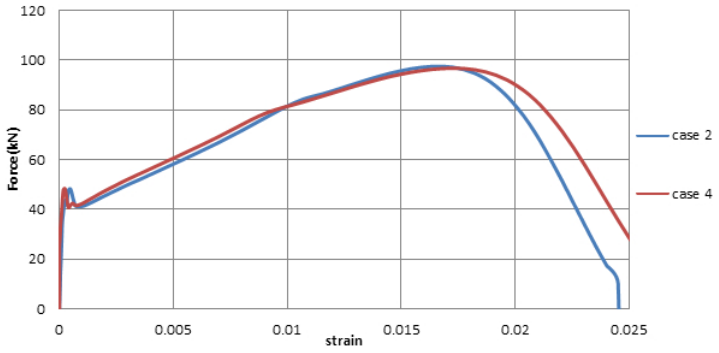

Figure 6.14: Comparison between case 2 and case 4

buckling happens earlier than case 2, but the maximum force happens later than case 2. As the difference is not large, the parameter will not influence the results a lot.

6.4 Influence of Lay Angle and Start Angle

In order to show the difference between the analytical solution and the test results, it is necessary to study and compare the results of different lay angles.

6.4.1 Lay Angle

Case 5. The property of the pipe model used in this case is: the lay angle is 26.5^0 and the start angle is 135^0. Other loading and boundary condition are the same as Case 1. The deformation and results are shown in Fig.6.15.

The same procedure is carried out the same as case 1, but the figure shows that there are four peaks along the curve, so it is the reason that the elements with the number 30031, 30074, 30110, 30157 with regard to the red circle in global element axial force curve are picked out to

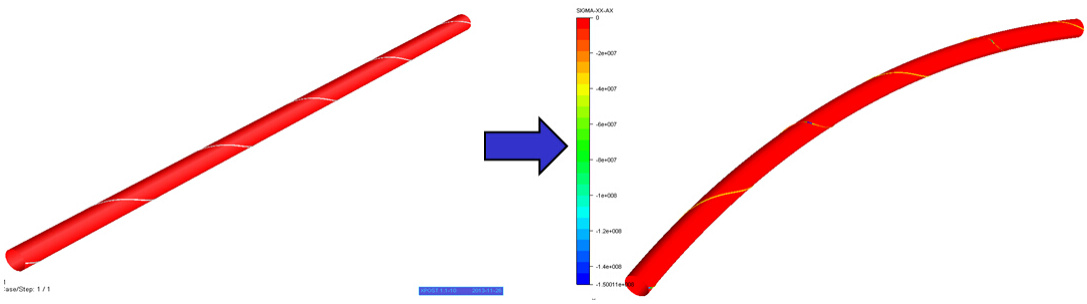

Figure 6.15: Deformation in the static and dynamic analysis case 5

study. The global element axial force at 60th second and the strain-force curves related to the elements according to the red circle are shown Fig.6.16.

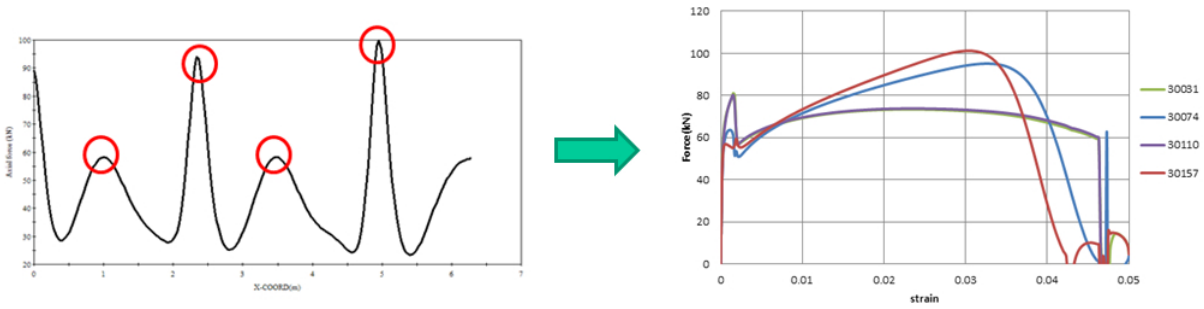

Figure 6.16: Global element axial force curve and strain-force curves, case 5

The maximum force should be multiplied by $\cos(26^0)$ when compared with the analytical solution. The buckling may happen in these four positions corresponding to four different buckling forces.

6.4.2 Start Angle

Theoretically, the start angle will not have any influence on the results. So the study of start angle is to show the sensitivity of this parameter in Bflex2010.

Case 6. The start angle is changed from 0 degree to 180 degree. The lay angle is the same as case 1. And the definition of start angle ψ is given in the Fig.6.17. The results are shown in Tab.6.1 and the middle element (30100) is picked out:

The curves are different among the five tests, and the reason is the start angle will decide the buckling position which will be different from one to another. The lateral buckling will lead to the change of the wire shape and if the middle element is picked out, it cannot decide whether

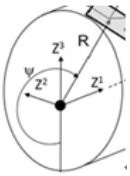

Figure 6.17: Definition of start angle

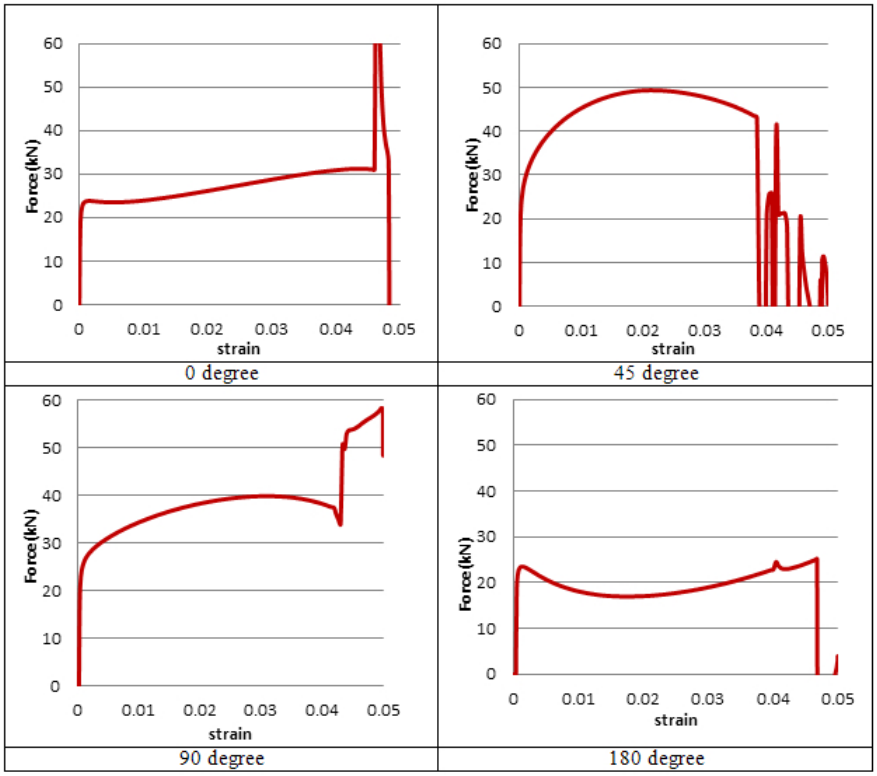

Table 6.1: Influence of start angle

the middle element is the expected element or not. So if the buckling behaviour of the middle element is studied, the curve of this element will be different.

6.5 Comparison With the Analytical Solution

6.5.1 Comparison Under the Lay Angle 35^0

The buckling force should be multiplied by a scale factor, in our case, the factor is 53. The comparison results are listed below:

The maximum buckling and post-buckling load happens comparison along the tendon among

the three cases and is shown in Fig.6.18 and the value is the axial force which should be multiplied by $\cos(35^0)$.

Firstly, as the load calculated from the formula 4.46 is the buckling load, the comparison between the buckling load of the test and the analytical results is done and shown in Tab.6.2. The first peak is due to the imperfection and the buckling load in the small red circle is the buckling load that is needed to pick out.

Buckling load	Case 1	Case 2	Case 3	Case 4
Test Results (kN)	–	33.4169	34.3647	34.4047
Analytical solution (kN)	66.0637	66.0637	66.0637	66.0637

Table 6.2: Comparison, buckling load

The analytical solution is bigger than the test results, which means the results given by Bflex2010 will be more conservative than the results from the analytical solution.

Secondly, the comparison post-buckling load between the test and analytical results is carried out and the results in the big red circle are picked out, which is shown in Tab.6.3.

Post-bucklng load	Case 1	Case 2	Case 3	Case 4
Test Results (kN)	84.8667	79.8427	80.6282	79.2224
Analytical solution (kN)	66.0637	66.0637	66.0637	66.0637

Table 6.3: Comparison, post-buckling load

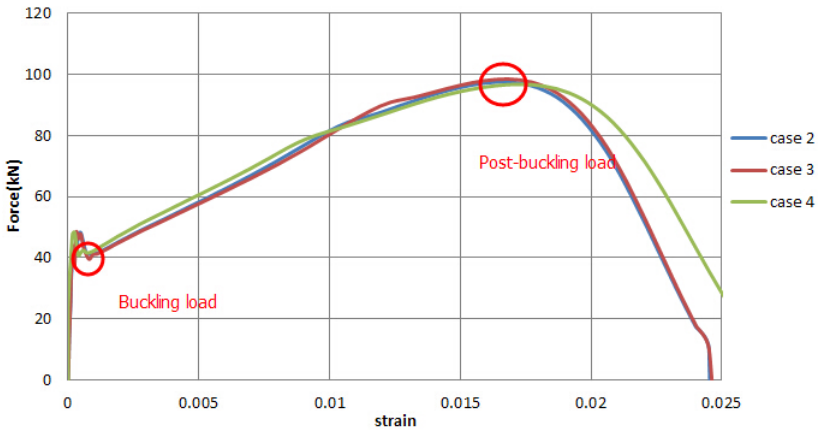

Figure 6.18: Maximum post-buckling load comparison

The difference among the three cases is small among the three cases, both for the maximum buckling load and post-buckling load. The results show that the analytical solution is smaller

than the test results for the post-buckling load, which means the analytical solution will be more conservative if it is applied as a critical value to approximate the post-buckling load.

6.5.2 Comparison Under the Lay Angle 26.2^0

For the case 5 which the lay angle is changed to 26 degree, the comparison results are listed in the Tab.6.4 associated with the results in Fig.6.19, where the results in the red circles are picked out as illustrated in the figure.

Lay angle 26.2	Maximum buckling load		Maximum post-buckling load	
Element	30031	30110	30074	30157
Test Results (kN)	46.9077	46.5718	78.3718	90.5119
Analytical solution (kN)	49.5928	49.5928	49.5928	49.5928

Table 6.4: Comparison between analytical and test results, case 5

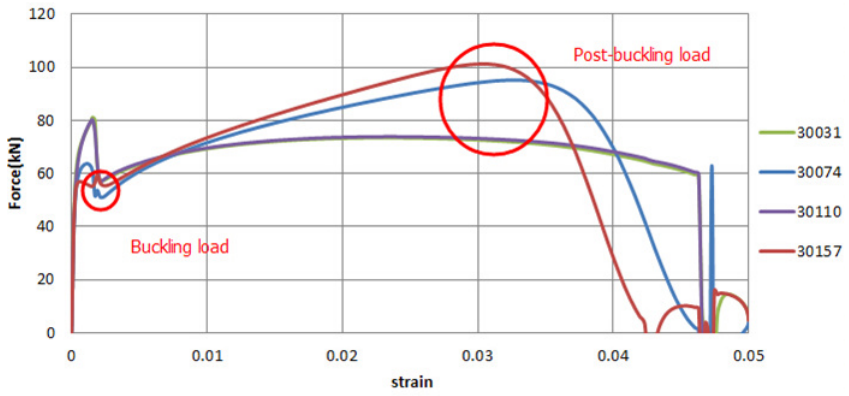

Figure 6.19: Maximum buckling and post-buckling load comparison, case 5

As it is shown in the table, for the tendon with a lay angle 26.2 degree, the results of buckling load from test will be little smaller but closer to analytical solution, which means the test results are conservative and accuracy in this case.

Chapter 7

BUCKLING PERFORMANCE OF FULL MODEL

7.1 Introduction

This chapter will represent the buckling analysis of the full model carried out in Bflex2010 and a comparison between the simplified and full model is carried out to study the influence of the anti-buckling tape and friction. The study of the influence of the anti-buckling tape and the lateral buckling behaviour due to the cyclic bending are also carried out, including a sensitivity analysis which will be done to study the lay angle influence of the anti-buckling tape. In addition, a comparison between the results from Bflex2010 and laboratory which was carried by Østergaard in 2012[4] will be preformed.

Fifteen cases in total are preformed in this chapter. The full model in case 1 has the same boundary and loading conditions as simplified model to perform the comparison between the two kinds of models. From case 2 to case 13 is to study the lateral buckling behaviour due to the cyclic bending with respect to three risers: 6 inch riser, 8 inch riser and 14 inch jumper, especially for the end rotation. Case 14 is to study the influence of anti-buckling tape. Case 15 is the sensitivity study associated with the effect of the lay angle of anti-buckling tape.

7.2 Lateral Buckling Analysis of Full Model

According to the same boundary and loading conditions, the analysis process will also be the same. Each tensile layer in full model includes four tendons, and 400 elements in total. Since the inner layer will suffer the lateral buckling first as explained in Chapter 4, the axial force with respect to x-coordinate is plotted to show the positions of buckling during the testing time. The position difference between buckling and post buckling should also be noticed.

7.2.1 Global and Local Buckling Analysis

Case 1. The model is based on the 6 inch riser with five layers and the lay angle is 26.2 degree. The buckling deformation of tensile layers is show in Fig.7.1.

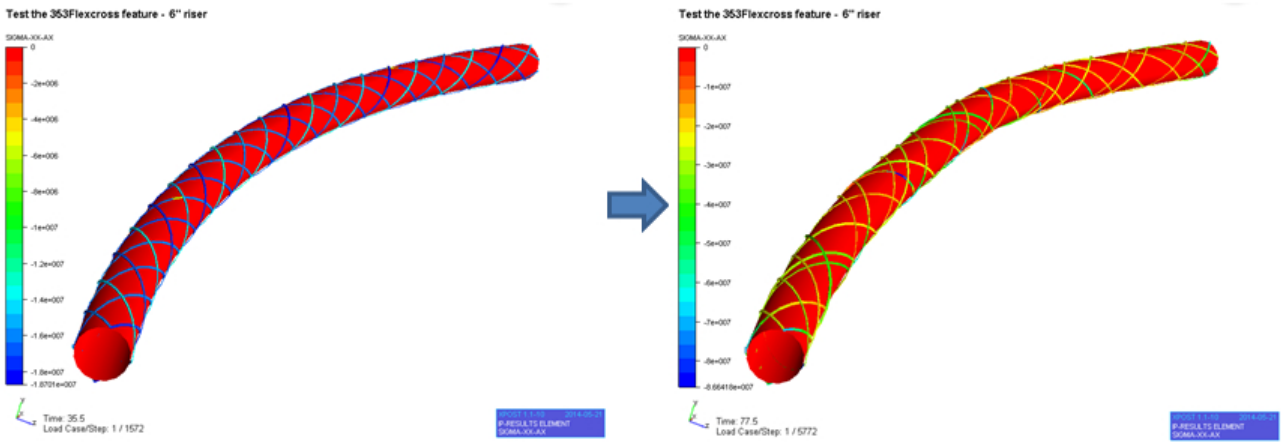

Figure 7.1: Buckling deformation of tensile layers

GLPLOT in Bflex2010 is used to show the relation of axial force and x-coordinate in terms of time. Figure.7.2 shows the change of global element axial force curve during buckling process.

The figures show the curve change from 40s to 47s which is the period of buckling process. The blue circle shows the position which loses the capacity first, but it is not a realistic situation because the sudden change doesn't influence the trend of the whole curve, so the reason must be the mistake during the computing process. Since it doesn't have any influence on the trend, the sudden change will be ignored.

The red circle shows the axial force change on the buckling position. The red circle position will suffer the buckling first, and the axial force will increase from 40s which is represented by

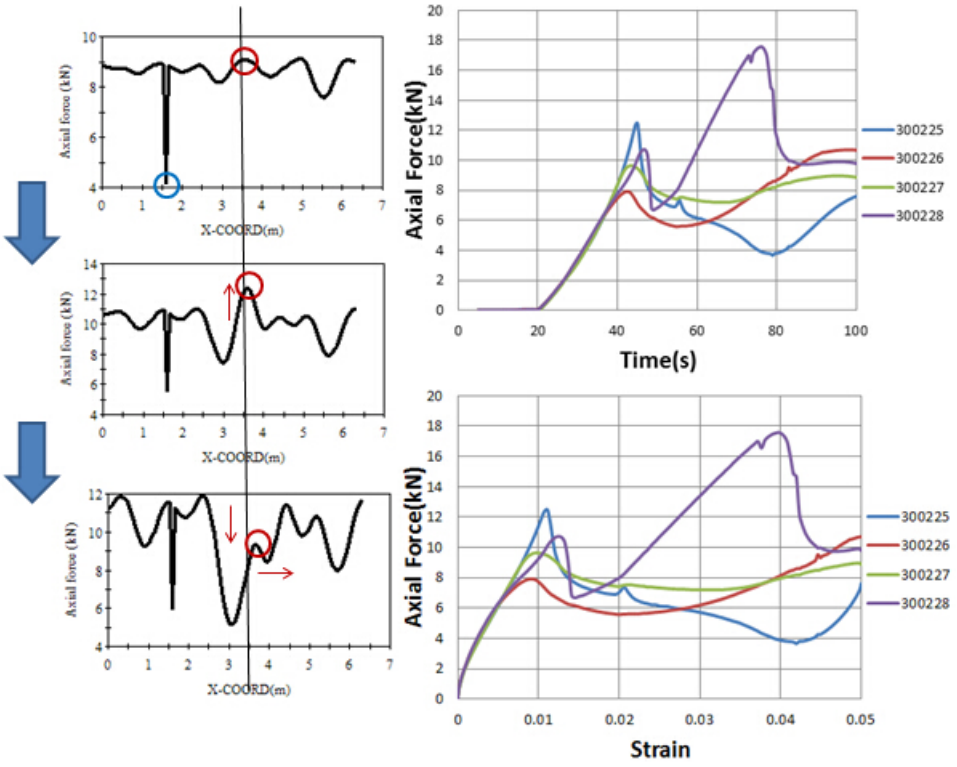

Figure 7.2: Global element axial force curve change during buckling process

the upward movement of the red circle. Then the red circle will move to right side which means there will be a lateral movement of the tendon. In addition, the circle will also have a downward movement which shows this part of tendon loses its capacity. And then there are other peaks occurring with higher value, which means there is not only one position that will buckle and there will be more buckling positions with even higher axial force. That is the reason why it is necessary to go through the pipe to find out the maximum axial force. However, in this section, the analysis will be performed by the first buckling position to study the transverse buckling behaviour. And then the maximum axial force bear by tendons will be given to compare with the analytical solution.

Since the tensile layer includes four tendons in the model to represent the whole layer, the results of the four tendons associate with the same cross-section should be added together and then multiplied by $\cos(26.2^0)$ to get the final axial loads. The elements 300225 to 300228 are in the same cross-section has the largest axial force associate with the time and are picked out to carry out the local analysis. The results fit the transverse buckling behaviour very well.

The analysis of post-buckling process is also based on the global analysis. After the buckling process, the steel will lose the capacity and induce a deformation. According to the elastic material stress-strain curve shown in Fig.7.3, the steel will extent its capacity to bear a larger load and then collapse.

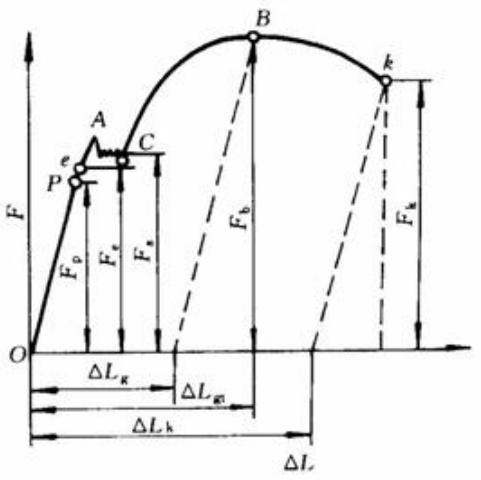

Figure 7.3: Elastic material stress-strain curve

From the global analysis, the position reference to the red circle will bear the largest stress. In the local analysis, elements 300243 to 300246 in one cross-section are picked out to study the post-buckling behaviour. The result is shown in Fig.7.4.

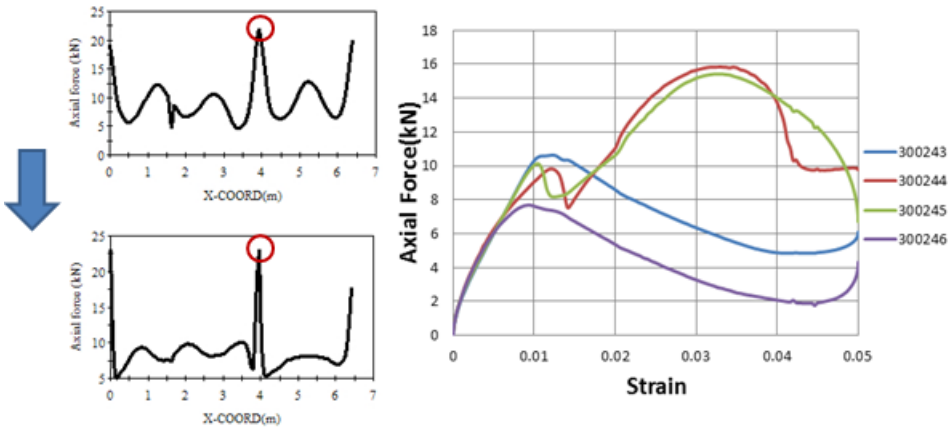

Figure 7.4: Global element axial force curve change during post-buckling process

The post-buckling force will keep on increasing after the first peak for the elements 300244

and 300245 and carry most of the axial load while the elements 300243 and 300246 will bear less axial load.

7.2.2 Comparison Between Simplified Model and Full Model

Since the lay angle for the tested full model is 26.2 degree, which is the same to the case 5 of the simplified model test, so the two cases are used to perform the comparison study. The comparison between these two models is shown in Fig.7.5.

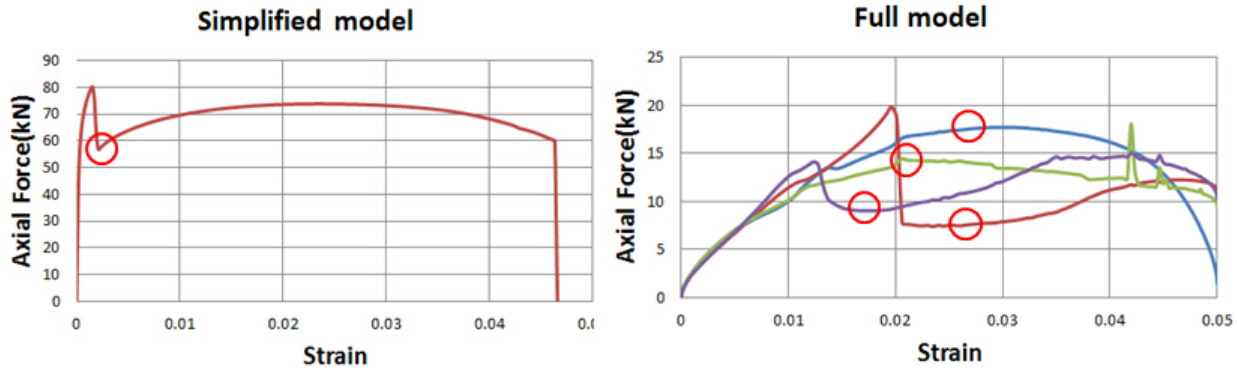

Figure 7.5: Comparison between simplified and full model

For the simplified model, the buckling happens very early because the model is built without friction and other layers. The influence of these is shown clearly in the full model. The buckling will start later around the strain 0.01, which means the pipe will be softer because of the composite structure, so the buckling will happen later during the process. After going through all the elements in the unit of cross-section, the maximum axial force acting on the inner tensile layer is shown in the Tab.7.1, which is also shown from the right side of the Fig.7.5 associated with the sum of the value in the four red circles.

Table.7.1 illustrates the data comparison between simplified and full model, with respect to the analytical solutions. The results of full model is from the element 300132 to 300135, within one cross-section which is more conservative compared with the simplified model because of the effect of the plastic tapes and the friction.

	Buckling load Bflex	Analytical solution
Simplified model	46.9077	49.8500
Full model	43.9723	47.8000

Table 7.1: Buckling load comparison between simplified and full model

7.3 Lateral Buckling Behaviour Due to Repeat Cycle Bending

7.3.1 Cases Overview

In this section, 12 cases are carried out to study the lateral buckling behaviour due to cyclic bending with respect to the experimental input data sheet which is shown in Tab.5.1 and the loading conditions for the 12 cases are shown in Tab.7.2 below:

Pipe ID	Case number	Applied compression (kN)	Bending radius (m)
6 inch riser, L=6.315m	2	265	11
	3	80	11
	4	210	11
	5	160	11
	6	265	8
14 inch jumper, L=11.235m	7	277	21
	8	269	8
	9	411	10
	10	950	12
8 inch riser, L=7.370m	11	300	12
	12	400	12
	13	700	12

Table 7.2: Test loading conditions in Bflex2010

The test pipe length is five times of the pitch length, which illustrated in the Tab.5.1. The axial stiffness of the pipes is obtained by fixing one end and adding a concentrate load at the end of pipe, then measuring the displacement of the end node and dividing the pipe length to get the strain. Then the axial stiffness can be calculated and shown in Tab.7.3.

According to the information in the data sheet, there are only four layers in the test pipes and the axial stiffness is not provided in the experiments. So the model is built based on the Tab.5.1 without the real axial stiffness applied in the experiments.

	6 inch riser	14 inch jumper	8 inch riser
Axial stiffness (MN)	159	210	143

Table 7.3: Axial stiffness of the three pipes

7.3.2 Analysis Process

The criteria of failure is when the steel loses its capacity. For the 6 inch riser, the wires are made by a basic grade steel with the yield strength of approximately 650Mpa. For the 8 inch riser and 14 inch jumper, the wires are made by a high strength grade steel with the yield strength of approximately 1350Mpa. If there are no failures, the rotation will be very small and increase slowly.

Case 2 is studied as an example for the process which is shown in Fig.7.6. To avoid the influence of the boundary conditions, the middle part of the pipe will be chosen to study. The red part of the tendon is the failure positions, where the stress carried by this part is bigger than the steel yield stress, so this part will collapse.

After that, the time when the red part appears will be selected to find the corresponding end rotation, which is shown in Fig.7.7. The explanation for the end rotation direction should be given as well. Since the inner tensile layer fails at first, in order to keep the torsion balance, the outer tensile layer will rotate following the direction of outer layer lay angle which results in the rotation of the whole pipe. For the test pipes, the lay angle is negative, so the end rotation will be negative as well.

Then the element 300163 which has the maximum longitude stress is picked out. As there are four corners in the tendon cross-section, and each corner has its own quantity, the results of the corner with maximum longitude stress σ_{xx} is selected and shown in Fig.7.8 with the corresponding yield stress 650MPa.

In addition, case 3 is studied as an no failure case example,shown in Fig.7.9 below. The stress in tendon will not surpass the yield stress of the steel, thus the rotation is very small and buckling will not happen.

Then the corner 3 of element 300201 which has the maximum longitude stress is picked out and shown in Fig.7.10. The longitude stress does not surpass the yield stress is 650MPa, which means there is no failure in the tensile layer during the process.

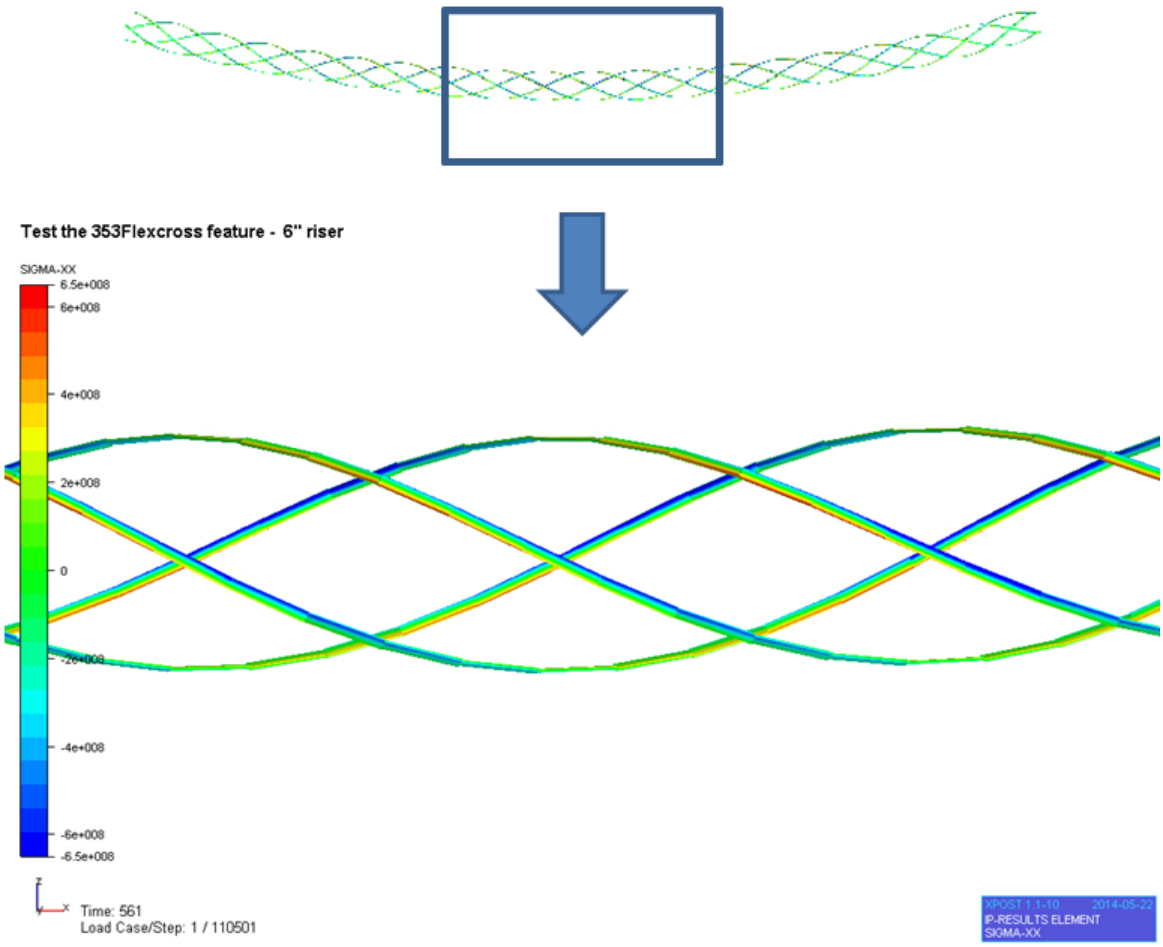

Figure 7.6: Example of the failure mode study process 1

7.3.3 Results of End Rotation

The results of the end node rotation are illustrated in Tab.7.4.

For the 6 inch riser, the yield stress of wires is smaller and the axial stiffness in the test may be also smaller compared with the experiment, so the pipe will collapse with a smaller end rotation. It will explain the reason why case 5 will collapse, which didn't collapse in experiment, and the smaller end rotation in the failure cases: case 2, case 4, case 6. However, for case 3 which the model suffers small compression, the test results fit the experimental results very well.

For the 14 inch jumper, the wires are made of high strength steel which the yield stress is bigger and the axial stiffness in the test may be close to the experiment, so the end rotations of the failure cases fit the experimental results quite well. However, the collapse of case 8 in Bflex also indicates the small axial stiffness used in test.

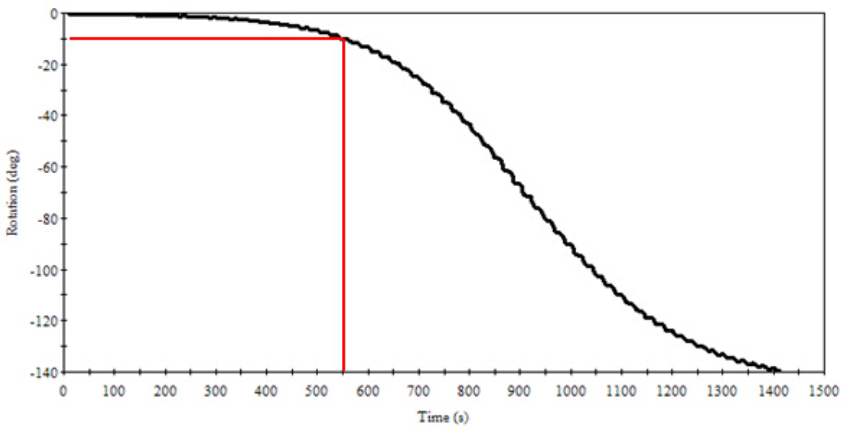

Figure 7.7: Example of the failure mode study process 2

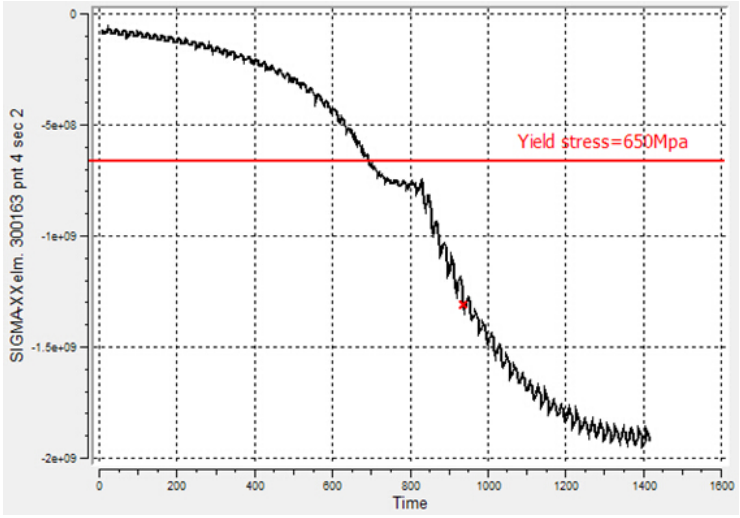

Figure 7.8: Longitudinal stress σ_{xx} in corner 4 of element 30163, case 2

For the 8 inch riser, the yield stress of wires is same as 14 inch jumper. The results of failure case 11 and no failure case 12, fit the experimental results very well. However, the test case 13 which is between the failure case and no failure case is unstable and the end rotation is increasing. While the experimental results of case 13 is also unstable and the end rotation is increasing slowly. So it is hard to say if the pipe will fail or not.

Since the axial stiffness is close to the realistic value for the four layers pipe structure used in experiments, the pipes tested in laboratory will have bigger axial stiffness , which may be provided by the added inner pipe to represent the influence of other layers, such as carcass and pressure layer.

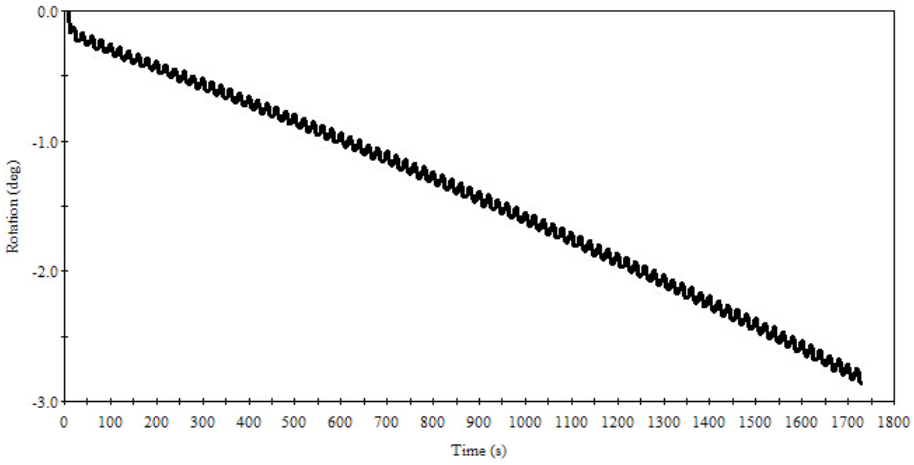

Figure 7.9: Example of the no failure case

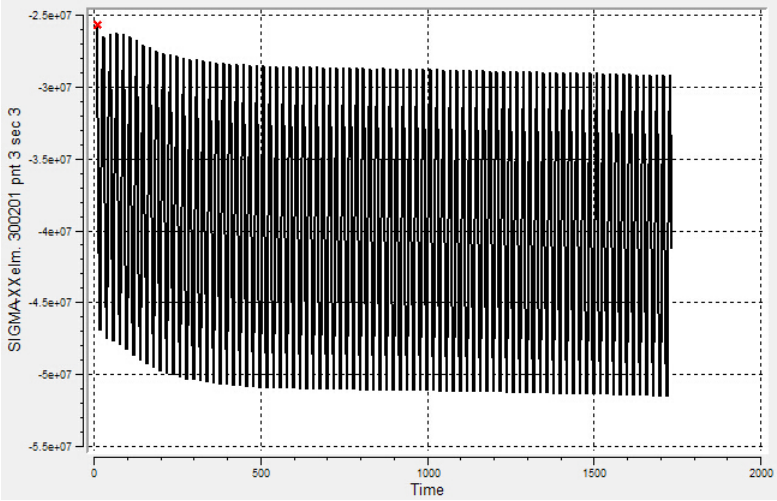

Figure 7.10: Longitudinal stress σ_{xx} in corner 3 of element 30201, case 3

7.4 Effect of Anti-buckling Tape

This section will study the effect of the anti-buckling tape to the lateral buckling behaviour. The sensitivity analysis is carried out to study the effect of anti-buckling tape and the influence of the direction of lay angle of anti-buckling tape .

7.4.1 Influence of Anti-buckling Tape

Firstly, the effect of anti-buckling tape is studied, and case 2 is selected to study the behaviour. Case 14 is based on case 2 to study this effect without the anti-buckling tape to be

Pipe ID	Case number	Applied compression (kN)	Bending radius (m)	Results in experiment	Pipe twist before unloading (deg)	Results in Bflex2010	Pipe twist before failure (deg)
6 inch	2	265	11	Failure	45 (increasing)	Failure	10 (increasing)
	3	80	11	No failure	<1 (stable)	No failure	3 (slowly increasing)
	4	210	11	Failure	45 (increasing)	Failure	11 (increasing)
	5	160	11	No failure	3 (slowly increasing)	Failure	3 (increasing)
	6	265	9	Failure	45 (slowly increasing)	Failure	10 (increasing)
14 inch	7	277	21	No failure	<1 (stable)	No failure	5 (slowly increasing)
	8	269	8	No failure	6.5 (increasing)	Failure	17 (increasing)
	9	411	10	Failure	27	Failure	27 (rapidly increasing)
	10	950	12	Failure	10 (rapily increasing)	Failure	11 (rapidly increasing)
8 inch	11	700	12	Failure	27 (slowly increasing)	Failure	21 (increasing)
	12	300	12	No failure	1	No failure	2.8 (slowly increasing)
	13	400	12	No failure	15 (slowly increasing)	Failure	18 (increasing)

Table 7.4: Results of pipe failure due to cyclic bending

compared with case 2. The results are shown in Fig.7.11, which shows clearly the important effect of anti-buckling tape to the lateral buckling behaviour. The slope of the two curves can show the anti-buckling tape can slow down the buckling process significantly. The slope of the pipe without anti-buckling tape is -0.272, while for the pipe with anti-buckling tape is -0.0112. The anti-buckling tape will slow down the buckling process by almost 20 times.

7.4.2 Influence of Lay Angle of the Anti-buckling Tape

Since the anti-buckling tape is rolled onto the pipe, it also has its own lay angle (usually around 85 degree) which will have influence to the pipe structure. In order to study the influence of the lay angle direction to the transverse buckling, a sensitivity study based on the case 9 will be performed to study this effect. The lay angle of anti-buckling tape is changed to +84.4 in the sensitivity case, case 15.

Figure.7.12 shows the effect of lay angle direction to the end rotation behaviour. Since the lay angle of the outer tensile layer is negative, the negative anti-buckling tape lay angle means

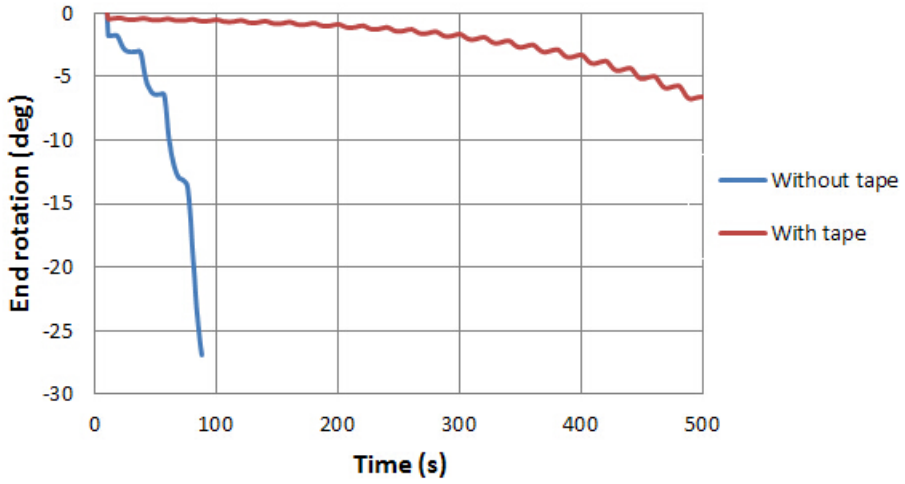

Figure 7.11: Comparison between the riser with and without anti-buckling tape

that it is in the same direction as the outer tensile layer. Whereas the positive lay angle means that it is in the different direction to the outer tensile layer.

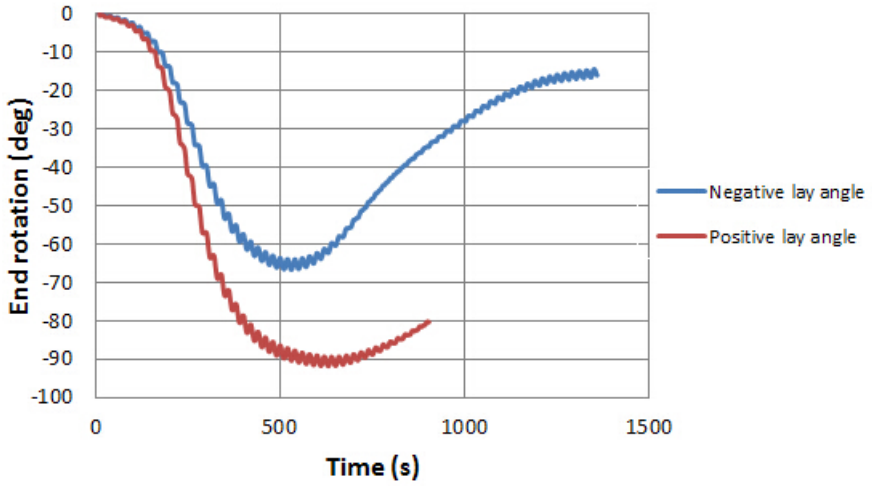

Figure 7.12: Comparison between the riser with negative and positive lay angle of anti-buckling tape

It should be noticed that there is a big difference between the two directions of lay angle. For the negative lay angle case, the slope of the dropping down part of the curve is -0.126 whereas -0.172 for the positive direction case. The negative lay angle direction will slow down the buckling process about 1.36 times. The results show the same direction between the outer tensile layer and anti-buckling tape will slow down the buckling process. In addition, for the negative lay angle case, after the failure, the inner and outer tensile layer will lose its capacity, and then the

pipe will twist back, which shows clearly the anti-buckling tape with this lay angle direction will contribute a lot to prevent the end rotation behaviour.

The stress, σ_{xx} in the anti-buckling tape is shown in Fig.7.14. It should be noticed that the definition of the direction σ_{xx} in the element HSHEAR363 is along the helix as shown in Fig.7.13.

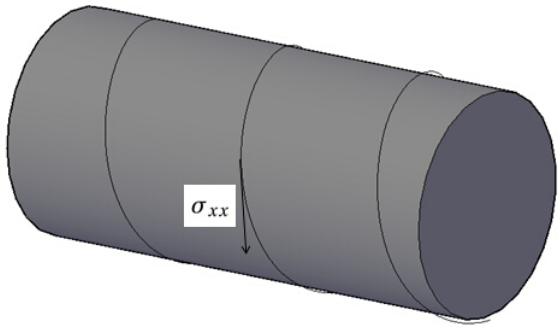

Figure 7.13: Definition of the σ_{xx} direction in element HSHEAR363

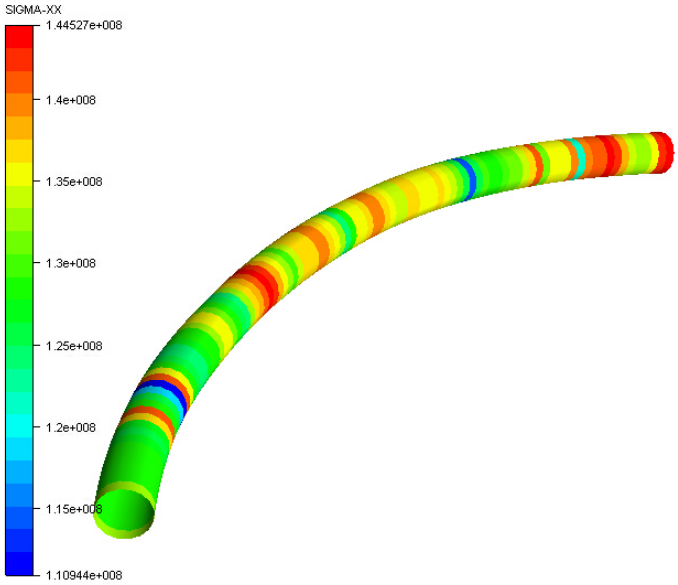

Figure 7.14: σ_{xx} in anti-buckling tape

Figure.7.14 shows clearly that the anti-buckling tape will bear the longitude stress which will also contribute to slow down the buckling process to a great extend. However, the σ_{xx} V.S time curve should also be given to prove this performance. In order to compare with the influence coming from the two different cases, the two curves are shown in Fig.7.15.

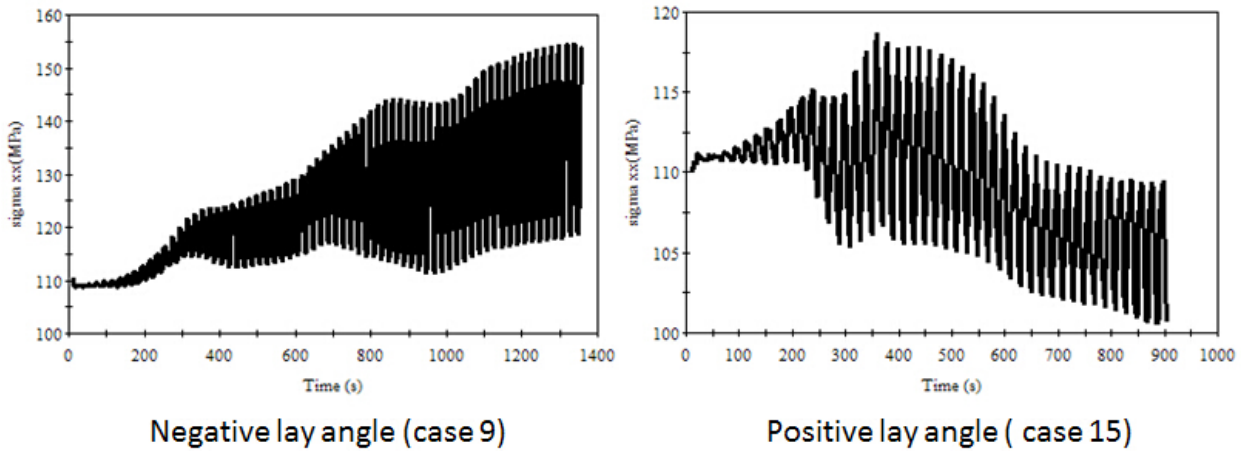

Figure 7.15: σ_{xx} comparison between the two cases

7.4.3 Results Analysis of Lay Angle Performance

The anti-buckling tape with the same lay angle as outer tensile layer will slow down the buckling process. What is more, the effect that the tape can contribute is increasing during the cyclic bending which can stop the end rotation and make the pipe twist to the normal position, which is shown in Fig.7.12. However, the other lay angle direction will keep on losing its preventing ability.

The reason is when the inner tensile layer lose its capacity first, the outer tensile layer will try to squeeze and twist in the direction of its own lay angle. Since the anti-buckling tape has the same lay angle direction as the outer tensile layer, the tape will also rotate to this direction which will make the tape squeeze tightly onto the layers below. Thus, this rotation behaviour will short the distance between the adjacent pitches and increase the corresponding compression, which will contribute more to the pipe to prevent the end rotation.

If the lay angle direction of the outer tensile layer and anti-buckling tape is different, the tape will also rotate, following the outer tensile layer, but the tape will become loose and keep losing its preventing ability.

Chapter 8

CONCLUSIONS AND RECOMMENDATIONS FOR FURTHER WORK

8.1 Summary and Conclusions

8.1.1 Summary

This master thesis has focused on the flexible pipeline and riser technology. The main purpose of this thesis is to study the transverse tensile armour buckling of flexible pipes, to establish the FE model to simulate the transverse buckling process and study the buckling performance as a function of lay angle , cross-section geometry, imperfection, and investigate the buckling behaviour due to different loading conditions, especially for the cyclic bending conditions. Another purpose is to study the influence of the anti-buckling tape to the transverse buckling, which is only applied to prevent the radial buckling of tensile layers before.

In this thesis, a brief introduction of the flexible pipe technology has been given, including an overview study of the failure modes and the design criteria. The theoretical background is also given, including a brief introduction of the finite element method as well as the non-linear finite element method and the relevant code study in FE software Bflex2010. The modelling method is also introduced, including the relative FE modelling theory used in Bflex2010 and the assumption of the method. Two FE models are established to study the transverse buckling of tensile armour, namely, a simplified model with one tendon and no friction to study the

buckling behaviour as the function of lay angle, cross-section geometry and the imperfection (loading condition) and a full model including all the layers and friction to study the transverse buckling behaviour due to the cyclic bending and the effect of the anti-buckling tape. A comparison between the analytical solution, experimental results and the test results in Bflex2010 is also performed.

8.1.2 Conclusions

Since the transverse buckling behaviour is studied by two models, the conclusions will be divided into two parts.

Simplified model

1. The lateral buckling of the tendon usually happens in the compression area.

2. The buckling area in tendon will produce high stress and lateral force. For the 35 degree lay angle, there will be only one peak during the process, following with the occurrence of buckling in this area.

3. The linear part of the force-strain curve of the core and tendon is symmetric to the X-axis, the lateral forces of the core and tendon are balanced each other.

4. The time increment is a key parameter in dynamic analysis in Bflex2010. With smaller time increment, the results will be more exact to the analytical value. The beginning of the buckling behavior and the correspondingly buckling load can be captured. The buckling load from tests will be smaller than that from the analytical solution.

5. The influence of axisymmetric shear interaction and the start procedure is relatively small compared with other parameters.

6. The start angle will have an influence on the position where the buckling happens in Bflex2010, but it has no influence on the analytical solution.

7. The comparison shows that for the tendon with a lay angle 35 degree, the results of buckling load from test will be smaller than the analytical solution and the post-buckling load will be larger than the analytical solution, which means the test results in Bflex2010 is conservative to use .

For the tendon with a lay angle 26 degree, the results of buckling load from test will be smaller and closer to the analytical solution, and the post-buckling load will be larger than that, which means the test results will be more conservative to apply for the small layer angle cases.

Full Model

1. The full model contains the plastic layers, tensile layers, anti-buckling tape, outer sheath and friction, which will make the pipe softer and allow the buckling to happen later under the same loading conditions as the simplified model.

The results from the full model is also close to the analytical results, which means the full model will also have the function to simulate the transverse buckling problem in a more conservative way, especially for predicting the relevant strain.

2. For cyclic bending problem, since the axial stiffness is not provided by the experiments, the axial stiffness used in test is smaller than the experiments, which means the tensile layer will buckle earlier than the experiments. However, it is also possible to use the value to investigate the transverse buckling behaviour which would be more conservative in the test.

The test results and the comparisons with experimental results show that the end of pipe will rotate as the predicted value in the theory part and the results are close to the experimental results, especially for the small compression no failure cases and the large compression failure cases.

3. The anti-buckling tape which is designed to prevent the radial buckling failure mode, will also have a great effect to slow down the buckling process.

The same lay angle direction between the outer tensile and anti-buckling tape will have better mechanism performance and increase the contribution to prevent the transverse buckling and the longitudinal stress which is carried by the anti-buckling tape will keep on increasing, specifically to inverse the end twist of the pipe. So this discovery will have important and significant effect on the design of the anti-buckling tape in flexible pipe.

8.2 Discussion

8.2.1 Discussion About Axial Stiffness

Since there is a difference between the test results and experiments results in cyclic bending cases and the reason has already been given, but a study of the influence of the axial stiffness should be carried out. As the axial stiffness in the model in Bflex2010 is calculated by the sum of different layers, it is actually more reliable in the real issue. However, the full model based on the data sheet only includes four layers and the relevant contact layers without the carcass and pressure layer. That may be the reason why the axial stiffness is relatively small as well as the small transverse buckling capacity of the tensile layer.

8.2.2 Discussion About Comparison Between Test and Analytical Solution

For the simplified model, the model contains one tendon to represent the whole tensile layer axial force, while in the full model, the axial force is represented by the four tendons which has the relevant movement respectively. So there will be some problems if the axial forces should be picked out within one cross-section. Another problem is because of the convergence rate. If the convergence rate is chosen to be small enough, the calculation will be more accuracy and the sudden increase can be avoid, but it will take much longer time to finish, which is not realistic in the practical issues. These two reasons make the results in the test in Bflex2010 larger, but these problems can be solved if the convergence rate is set to be smaller and the elements are rightly chosen by taking the relative movements. However, even if the test results are a litter higher than the analytical solution, it can also be used to predict the transverse buckling behaviour, such the buckling position, end rotation, maximum buckling and post-buckling loads and the stress distribution in the plastic layers and anti-buckling tape.

8.3 Recommendations for Further Work

For the transverse buckling study carried out by simplified model and the relevant cases by full model, the way to increase the accuracy of the calculation is to choose a relatively small convergence rate.

For the transverse buckling behaviour caused by cyclic bending, the axial stiffness of the experimental pipe should be given and correlated to test results carried out in this thesis. If the stiffness is rightly chosen, the test results will be closer to the experiments results.

Another important case study should also be performed to investigate the influence of the material of anti-buckling tape contributing to the ability to restrain the transverse buckling. And the influence of the material, lay angle and tape cross-section of anti-buckling tape should also be studied to optimize the flexible pipe design.

REFERENCES

[1] S. Berge, A. Engseth, I. Fylling, C.M. Larsen, B.J. Leina, T. Nygaard, and Olufesn A. Handbook on design and operation of flexible pipes, 1992.

[2] P. Secher, F. Bectarte, and A. Felix-Henry. Lateral buckling of armor wires in flexible pipes: reaching 3000 m water depth. Proceedings of OMAE, 2011.

[3] S. Sævik. *Offshore Pipeline Technology*. 2013.

[4] N.H. Østergaard, A. Lyckegaard, and J. Andreasen. A method for prediction of the equilibrium state of a long and slender wire on a frictionless toroid applied for analysis of flexible pipe structures. Engineering Structures, Vol. 34, pp. 391-399,2012.

[5] Wang Chuan, Hongwu Zhu, and Dingya Wang. Test system and model for fatigue performance evaluation of marine riser. Journal of Applied Seiences 13(6): 854-861, 2013.

[6] API RECOMMENDED PRACTICE 17B. In recommended practice for flexible pipe. american petroleum institute. 3rd edition, 2002.

[7] Niels Højen Østergaard. *On lateral buckling of armouring wires in flexible pipes*. PhD thesis, Aalborg University/NKT-Flexibles, Aalborg East, Denmark, 2012.

[8] M.P. Braga and P Kaleff. Flexible pipe sensitivity to birdcaging and armor wire lateral buckling. Proceedings of OMAE, 2004.

[9] N.H. Østergaard, A. Lyckegaard, and J. Andreasen. Simplified approaches to modeling of lateral wire buckling in the tensile armour of flexible pipes. Proceedings of OMAE, 2012.

[10] N.H. Østergaard, A. Lyckegaard, and J. Andreasen. On lateral buckling failure of armour wires in flexible pipes. Proceedings of OMAE, 2011.

[11] S. Sævik. BFLEX2010 - *Theory Manual*. MARINTEK, Trondheim, Norway, 2010.

[12] S. Sævik, O. D. Økland, G. S. Baarholm, and J. Gjøsteen. BFLEX2010 - *Users Manual*. MARINTEK, Trondheim, Norway, 2009. Marintek Document.

[13] API Spec 17J. Specification for unbonded flexible pipes. american petroleum institute. 3rd edition, 2008.

[14] T.Moan. *Finite Element Modelling and Analysis of Marine Structure*. 2003, Department of Marine Technology, NTNU.

[15] S. Sævik. *On Stresses and Fatigue in Flexible Pipes*. PhD thesis, NTH, Trondheim, Norway, 1992.

[16] S. Sævik. A finite element model for predicting stresses and slip in flexible pipe armouring tendons. *Computers and Structures*, 46(2):219 – 230, 1993.

[17] S. Sævik. Theoretical and experimental studies of stresses in flexible pipes. *Computers and Structures*, 89(23):2273 – 2291, 2011.

[18] S. Sævik and Guomin Ji. Differentiate equation for evaluation transverse buckling behavior of tensile armor wires. Proceedings of OMAE, 2014.

Appendix A

Model Code in Bflex2010

This section will give the model code of the two models established in Bflex2010. All the cases are based on these two codes with some certain relevant changes.

A.1 Simplified Model

```
HEAD BFLEX2010 - Buckling
#-------------------------------------------------------------------------
# Control data
#         maxit  ndim  isolvr npoint ipri  conr  gacc    iproc
CONTROL    100    3    2      16    01  1.e-5   0.0    stressfree
DYNCONT      2   0.0 0.09   -0.05
#-------------------------------------------------------------------------
# Nocoor input
#                   no       x     y     z
Nocoor Coordinates
             1       0.0       0.0    0.0
           201       6.315    0.0    0.0
# 1st structural layer
#      no      x0    y0   z0   b1   b2   b3       R node    xcor  theta
Nocoor Polar  0.0   0.0  0.0  0.0  0.0  0.0  0.0991 30001 0.00   0.0000+2.3562
                                                   30201 6.315  44.6197+2.3562
Visres Integration 1 sigma-xx Sigma-xx-ax Sigma-xx-my Sigma-xx-mz Vconfor-z
#-------------------------------------------------------------------------
# Elcon  input
# The core
#      group       elty       material  no  n1     n2  n3   n4
Elcon  core        pipe31     plastic  1   1      2
#       n   elinc  nodinc
Repeat 200   1        1
# Tensile Layer 1
#      group         elty   flexcrossname     no   n1    n2     n3     n4
Elcon  tenslayer1 hshear353   tendon    30001   1      2    30001   30002 repeat 200 1 1
#-------------------------------------------------------------------------
# Orient input
# The core
#                     no     x  y    z
```

```
Elorient Coordinates    1      0  1e3    0
                        200    0  1e3    0
#                      no     x  y    z
# Tensile Layers
#                      no     x  y    z
Elorient Coordinates  30001     0  1e3    0
                      30200     0  1e3    0
#-------------------------------------------------------------------
# Element property input
#         name        type    rad  th  CDr  Cdt  CMr  CMt        wd       ws    ODp  ODw rks
ELPROP    core        pipe  0.0976  0.001    1.0  0.1  2.0  0.2 500.00 0.00  0.197  0.197 0.5
#                                      b      t      md   ms   scale     thims thimd  iop
ELPROP tenslayer1   shearhelix rectangle 0.010  0.003    0.2  0.0  53.0   200   100    0 d d d d
#                                 gap0 tunetime gaplogic AUTOMNPC transformation scalefac
#          name   type        shearm
# Boundary condition data
#      Loc    node  dir
BONCON GLOBAL 1      1
BONCON GLOBAL 1      2 repeat 201 1
BONCON GLOBAL 1      3
BONCON GLOBAL 1      4 repeat 201 1
BONCON GLOBAL 1      6 repeat 201 1
BONCON GLOBAL 201    3
# fix the relative disp at ends
BONCON gLObAL 30001      1
BONCON gLObAL 30001      2
BONCON gLObAL 30001      3 repeat 201 1
BONCON gLObAL 30001      4 repeat 201 1
BONCON gLObAL 30201      1
BONCON gLObAL 30201      2
#-------------------------------------------------------------------------------
#  Material data
#        name      type      poiss talfa     tecond  heatc  beta ea    eiy     eiz      git      em     gm     den
MATERIAL plastic   linear    0.0   11.7e-6   50   800   0    3.67e10 3.210e12 3.210e12 2.50e12   2.1e11  8e10  1000 2.1e11
MATERIAL tendon    elastic   0.3   7850 11.7e-6   50   800   2.1e11 8.076e10 2.1e11
#        name     type           alfa poiss ro      talfa    tecond  heatc eps sigma
TIMECO      20.0     1.    1.0    100.0  static       auto     go-on   disp    50      5      1e-5
TIMECO     100.0     0.005   0.5    100.0  dynamic      auto     none    disp    30      5      1e-4
#-----------------------------------------------
# load input
#     hist  dir  no1 r1  no2 r2         n m
inistr  400     1     30001  -0.025 30200 -0.025
inistr  500     5     1  -0.0909 200 -0.0909
inistr  600     6     30001   0.001  30200 0.001
#-----------------------------------------------
PELOAD 200 100
#-----------------------------------------------------------
# force
# drymass
 THIST 100  0          1.0
            1          1.00
           10          1.00
           20          1.00
# buoyancy
 THIST 200  0          0.0
            1          0.00
           10          0.00
           20          0.00
          100          0.00
# inistr x-dir
THIST_R 400  0.0          20.0 rampcos 0.0
             20.0         100.0 rampcos 2.0
```

```
# inistr curvature
 THIST_R 500  0.0          10.0 rampcos 0.0
             10.0          20.0 rampcos 1.0
#initial curvature
 THIST_R 600  0.0          10.0 rampcos 0.0
```

A.2 Full Model

```
HEAD Test the 353Flexcross feature -  6" riser
#-------------------------------------------------------------------------
# Control data
#         maxit  ndim  isolvr npoint ipri  conr  gacc    iproc
CONTROL    500    3    2      16    01  1.e-9   0.0    restart 1
#       Matat  Alpha1  Alpha2  Alpha
DYNCONT  1      0.0     0.09   -0.05
#-------------------------------------------------------------------------
#
# Nocoor input
#
#            no      x         y      z
Nocoor Coordinates
             1        0.0       0.0    0.0
             101      6.315       0.0    0.0
#  core
#             no         x         y      z
Nocoor Coordinates
             10001       0.0       0.0    0.0
             10100       6.252     0.0    0.0
# anti-wear
#             no         x         y      z
Nocoor Coordinates
             20001       0.0       0.0    0.0
             20100       6.252     0.0    0.0
# anti-birdcaging and outersheath
#             no         x         y      z
Nocoor Coordinates
             30001       0.0       0.0    0.0
             30100       6.252     0.0    0.0
# tensile-1
#      no      x0    y0   z0   b1   b2   b3       R node    xcor  theta
Nocoor Polar  0.0   0.0  0.0  0.0  0.0  0.0  0.1005
300001 0.00  0.0
300101 6.315   30.919
#      N      Nodeinc   Xinc    Thetainc
Repeat 4     101        0.0     0.392*4
# tensile-2
#      no      x0    y0   z0   b1   b2   b3       R node    xcor  theta
Nocoor Polar  0.0   0.0  0.0  0.0  0.0  0.0  0.1045
400001 0.00  0.0
400101 6.315   -29.7356
#      N      Nodeinc   Xinc    Thetainc
Repeat 4     101        0.0     0.392*4
#
Visres Integration 1 Sigma-xx-ax Sigma-yy Vconfor-z sigma-xx sigma-xx-my sigma-xx-mz
#-------------------------------------------------------------------------
# Elcon  input
# Structural layers
#      group       elty       material      no     n1     n2  n3   n4
#Elcon  carcass        hshear363  mypipe     1       1      2   10001 repeat 100 1 1
Elcon  core           hshear363  mypipe     1       1      2   10001 repeat 100 1 1
```

```
Elcon  pipe           pipe31     pipemat    1001    1      2   repeat 100 1 1
Elcon  strutape       hshear363  mypipe     10001   1      2   20001 repeat 100 1 1
Elcon  buckling       hshear363  mypipe     20001   1      2   30001 repeat 100 1 1
Elcon  outersheath    hshear363  mypipe     30001   1      2   30001 repeat 100 1 1
Elcon  tensile1       hshear353  mypipe     300001  1      2   300001 300002
                                            300004  1      2   300304 300305 repeat 100 4 1
Elcon  tensile2       hshear353  mypipe     400001  1      2   400001 400002
# Contact layers
Elcon  corecontact         hcont463   mypipe    500001   10001     300001   300002
                                               500004   10001     300304   300305 repeat 100 4 1
Elcon  tapeoutwardcontact  hcont463   mypipe    510001   300001    300002   20001
                                               510004   300304    300305   20001  repeat 100 4 1
Elcon  tapeinwardcontact   hcont463   mypipe    520001   20001     400001   400002
                                               520004   20001     400304   400305 repeat 100 4 1
Elcon  antiincontact       hcont463   mypipe    530001   400001    400002   30001
#       n   elinc  nodinc
#-------------------------------------------------------------------------
# Orient input
# structural els
#                      no        x     y     z
Elorient Coordinates    1        0    1e3    0
                        100      0    1e3    0
Elorient Coordinates    1001     0    1e3    0
                        1100     0    1e3    0
Elorient Coordinates    10001    0    1e3    0
                        10100    0    1e3    0
Elorient Coordinates    20001    0    1e3    0
                        20100    0    1e3    0
Elorient Coordinates    30001    0    1e3    0
                        30100    0    1e3    0
Elorient Coordinates    300001   0    1e3    0
                        300400   0    1e3    0
Elorient Coordinates    400001   0    1e3    0
                        400400   0    1e3    0
# contact
elorient eulerangle     500001   0.0   0.0   0.0
                        500400   0.0   0.0   0.0
elorient eulerangle     510001   0.0   0.0   0.0
                        510400   0.0   0.0   0.0
elorient eulerangle     520001   0.0   0.0   0.0
                        520400   0.0   0.0   0.0
elorient eulerangle     530001   0.0   0.0   0.0
                        530400   0.0   0.0   0.0
#-------------------------------------------------------------------------------
#              name          type      ID         Timeini    ilaint ilaext ielbfl fimod     content   nelgr   el1   el2
CROSSECTION  mypipe  353FLEXCROSS     194e-3     10.1         2      6      1     0     1000    6
1-1-corecontact-core
2-2-tapeoutwardcontact-tensile1
3-3-strutape-tapeinwardcontact
4-4-antiincontact-tensile2
5-5-buckling
6-6-outersheath
#FLEXBODY A=5*12.7*.563 = 36.0, FLEXLOK A=6.4*14.1*.878 = 79.23
#  CTYPE    TH     matname       FRIC   LAYANG  RNUM  TEMP     nlmat      CCODE      CFATFL  AREA      IT          INY          IKS       WIDTH
    THER   2.0e-3    plast_PA11    0.15   0.000     0    0.0      none       NONE          NONE   0.00   0.000e+00   0.000e+00   0.000e+00     0.00
# 1st armour
    TENS   3.00e-3   steel_190     0.15   26.2      52   0.0      steel_190 FLEXTENSILE   NONE   0.00   0.000e+00   0.000e+00   0.000e+00     0.00
    THER   1.00e-3   plast_PA11    0.15   0.000     0    0.0      none       NONE          NONE   0.00   0.000e+00   0.000e+00   0.000e+00     0.00
# 2nd armour
    TENS   3.00e-3   steel_190     0.15   -26.2     54   0.0      steel_190 FLEXTENSILE   NONE   0.00   0.000e+00   0.000e+00   0.000e+00     0.00
    TAPE   1.00e-3   glass_fil     0.15   83.5      1    0.0      none       MYTAPE        NONE   0.00   0.000e+00   0.000e+00   0.000e+00     0.00
    THER   6.0e-3    rubber        0.15   0.000     0    0.0      none       NONE          NONE   0.00   0.000e+00   0.000e+00   0.000e+00     0.00
```

```
#CROSS-SECTION BOUNDARY DATA
#             NAME       type  X0  Y0   CCURV    P1         P2      P3       P4      NINTER    ICODE
#
CROSSGEOM TENS-FLEXTENSILE  BFLEX 0 0  S      0.01      0.0000   0.0000   0.0000      30     1
                                       S     0.003     90.0000   0.0000   0.0000      20     1
                                       S      0.01    180.0000   0.0000   0.0000      30     1
                                       S     0.003    270.0000   0.0000   0.0000      20     1
CROSSGEOM  TAPE-MYTAPE      BFLEX 0 0  S      0.06      0.0000   0.0000   0.0000      30     1
                                       S     0.001     90.0000   0.0000   0.0000      20     1
                                       S      0.06    180.0000   0.0000   0.0000      30     1
                                       S     0.001    270.0000   0.0000   0.0000      20     1
ELPROP   pipe   pipe  0.05  0.001    1.0  0.1  2.0  0.2 0.00 0.00  0.152  0.152 0.5
#-------------------------------------------------------------------------
# Boundary condition data
#      Loc    node  dir
BONCON GLOBAL 1      1
BONCON GLOBAL 1      2
BONCON GLOBAL 1      3
BONCON GLOBAL 1      4
BONCON GLOBAL 1      6
BONCON GLOBAL 101      2
BONCON GLOBAL 101      3
# fix the relative disp at ends
BONCON gLObAL 300001      1 repeat 4 101
BONCON gLObAL 300001      2 repeat 4 101
BONCON gLObAL 300001      4 repeat 404 1
BONCON gLObAL 300001      5 repeat 404 1
BONCON gLObAL 300101      1  repeat 4 101
BONCON gLObAL 300101      2  repeat 4 101
# fix the relative disp at ends
BONCON gLObAL 400001      1 repeat 4 101
BONCON gLObAL 400001      2 repeat 4 101
BONCON gLObAL 400001      4 repeat 404 1
BONCON gLObAL 400001      5 repeat 404 1
BONCON gLObAL 400101      1  repeat 4 101
BONCON gLObAL 400101      2  repeat 4 101
#
BONCON gLObAL 10001      2 repeat 100 1
BONCON gLObAL 10001      3 repeat 100 1
BONCON gLObAL 20001      2 repeat 100 1
BONCON gLObAL 20001      3 repeat 100 1
BONCON gLObAL 30001      2 repeat 100 1
BONCON gLObAL 30001      3 repeat 100 1

TIMECO      10.0     10.0    1.0    100.0  static       auto     none   disp    10      5      1e-5
TIMECO      11.0     0.002   1.0    100.0  dynamic      auto     none    disp    20      10      1e-5
TIMECO     2460.0    0.005   2.0    100.0  dynamic      auto     none    disp    20      10      1e-5
#---------------------------------------------
# load input
#
PELOAD  100   100
#     hist  dir  no1 r1  no2 r2         n m
inistr  200     1     1001    2.65   1100   2.65
constr pdisp global   1 5  0.395 300
constr pdisp global 101 5 -0.395 300
#-------------------------------------------------------------------------------------
# mass
THIST 100  0.0       1.0
           0.5       1.0
# inistr
THIST_R 200    0.0     10.0    rampcos 1.0
#---------------------------------------------
```

```
# inistr x-dir
 THIST_R 300    0.0     10.0    rampcos 0.0
               10.0     20.0    rampcos 1.0
               20.0     30.0    rampcos 0.0
               30.0     40.0    rampcos 1.0
              ...
             2440.0   2450.0    rampcos 1.0
             2450.0   2460.0    rampcos 0.0
#-------------------------------------------------------------------------
#  Material data
#        name         type     poiss  talfa    tecond   heatc  beta ea    eiy   eiz    git    em        gm      den   Etrans
MATERIAL pipemat      linear    0.3   11.7e-6   2.0     50     800   1e5  0     0    0  2.00E11    0.8e11   8E3  2.00E11
MATERIAL steel_190    linear    0.3   11.7e-6   2.0     50     800   0    0     0    0    2.1E11    0.8e11   8E3  2.1E11

#
MATERIAL plast_PA11   linear    0.35  11.7e-6   2.0     50     800   0    0     0    0    179e6       100.0e6    1E3  1179e6
MATERIAL glass_fil    linear    0.4  11.7e-6   2.0     50     800   0    0     0    0    27e9       1000.0e6  1E3   27e9
MATERIAL rubber       linear    0.4  11.7e-6   2.0     50     800   0    0     0    0    400e6       1000.0e6   1E3   400e6
```

Appendix B

End Rotation, Case 4 to Case 13

This section includes the end rotation results of the rest cases from case 4 to case 13.

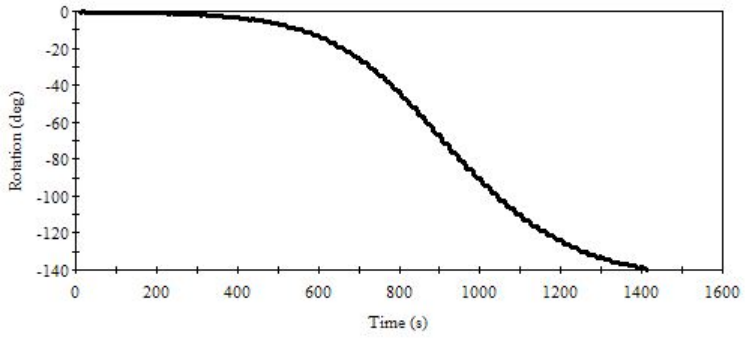

Figure B.1: End rotation, case 4

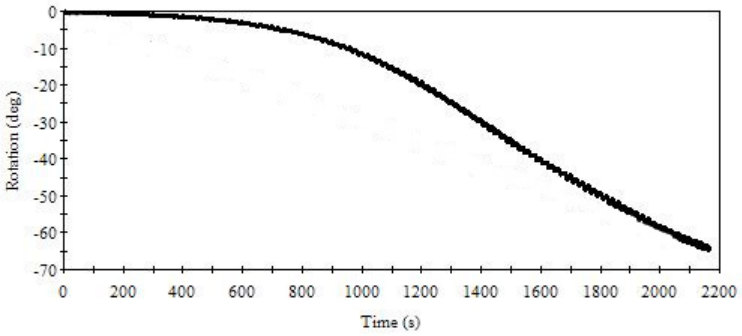

Figure B.2: End rotation, case 5

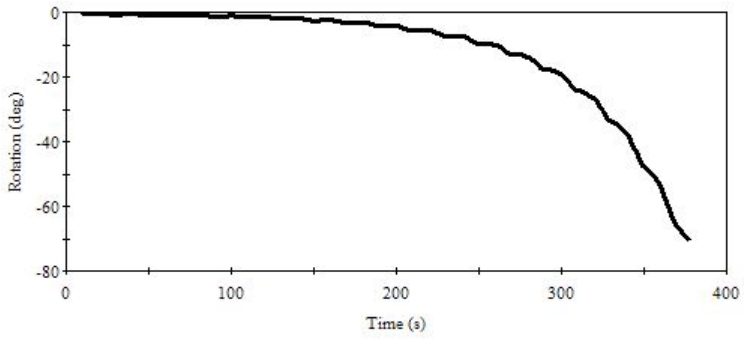

Figure B.3: End rotation, case 6

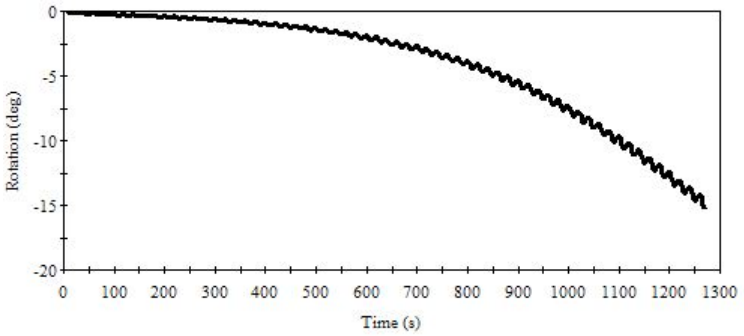

Figure B.4: End rotation, case 7

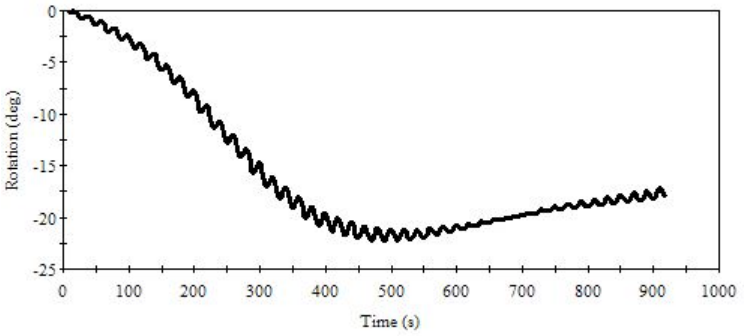

Figure B.5: End rotation, case 8

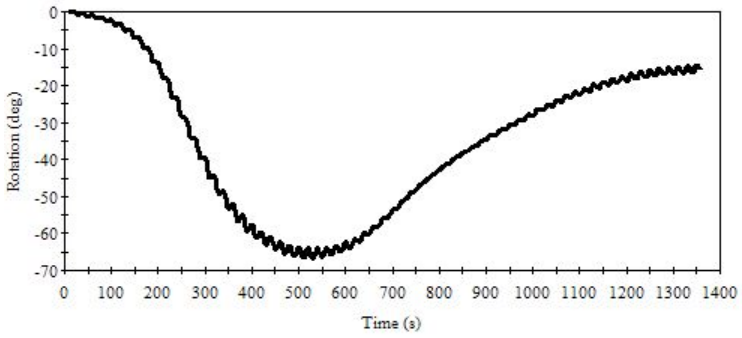

Figure B.6: End rotation, case 9

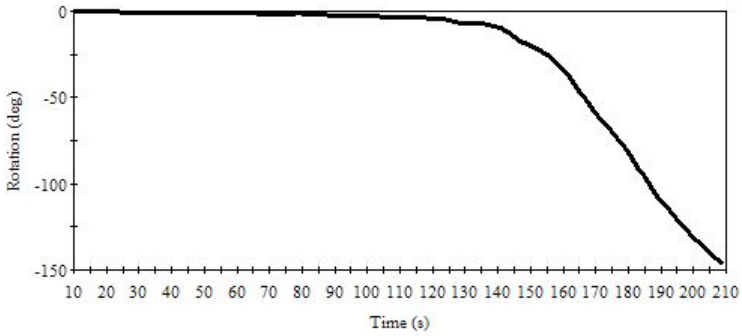

Figure B.7: End rotation, case 10

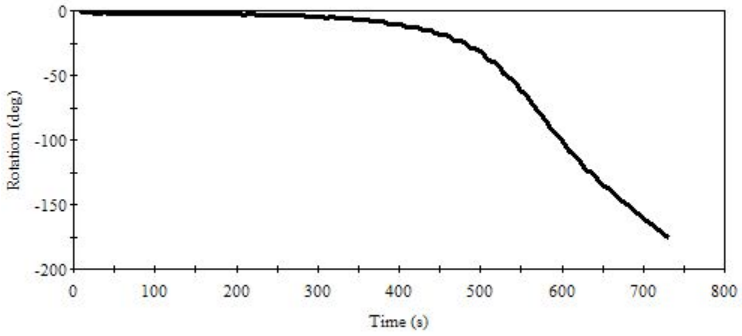

Figure B.8: End rotation, case 11

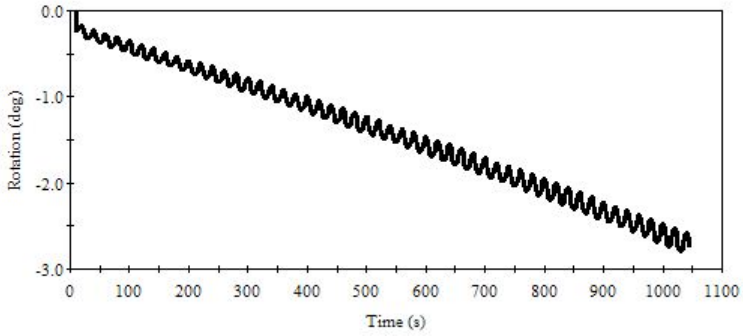

Figure B.9: End rotation, case 12

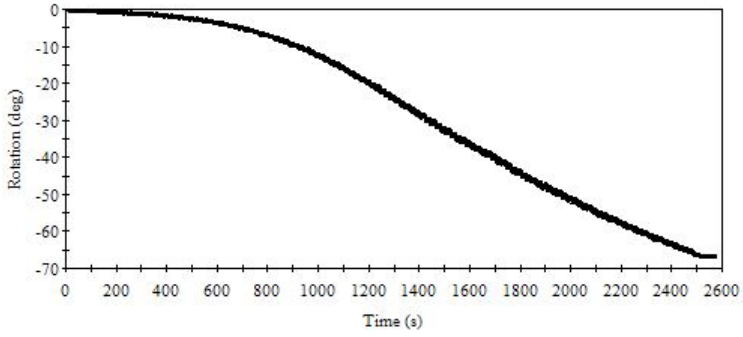

Figure B.10: End rotation, case 13